

**Nonsingular bounce cosmology from Lagrange multiplier  $F(R)$  gravity**Shin'ichi Nojiri,<sup>1,2,\*</sup> S. D. Odintsov,<sup>3,4,5,†</sup> V. K. Oikonomou<sup>6,5,7,‡</sup> and Tanmoy Paul<sup>8,§</sup><sup>1</sup>*Department of Physics, Nagoya University, Nagoya 464-8602, Japan*<sup>2</sup>*Kobayashi-Maskawa Institute for the Origin of Particles and the Universe,  
Nagoya University, Nagoya 464-8602, Japan*<sup>3</sup>*Institució Catalana de Recerca i Estudis Avançats, Passeig Lluís Companys, 23, 08010 Barcelona, Spain*<sup>4</sup>*Institut de Ciències de l'Espai-Consejo Superior de Investigaciones Científicas,  
C. Can Magrans s/n, 08193 Barcelona, Spain*<sup>5</sup>*International Laboratory for Theoretical Cosmology, Tomsk State University of Control Systems  
and Radioelectronics (TUSUR), 634050 Tomsk, Russia*<sup>6</sup>*Department of Physics, Aristotle University of Thessaloniki, Thessaloniki 54124, Greece*<sup>7</sup>*Tomsk State Pedagogical University, 634061 Tomsk, Russia*<sup>8</sup>*Department of Theoretical Physics, Indian Association for the Cultivation of Science,  
2A & 2B Raja S.C. Mullick Road, Kolkata—700 032, India*

(Received 19 July 2019; published 25 October 2019)

In this work, we study nonsingular bounce cosmology in the context of the Lagrange multiplier generalized  $F(R)$  gravity theory of gravity. We specify our study by using a specific variant form of the well-known matter bounce cosmology, with scale factor  $a(t) = (a_0 t^2 + 1)^n$ , and we demonstrate that for  $n < 1/2$ , the primordial curvature perturbations are generated deeply in the contraction era. Particularly, we show explicitly that the perturbation modes exit the horizon at a large negative time during the contraction era, which in turn makes the “low-curvature” regime, the era for which the calculations of observational indices related to the primordial power spectrum can be considered reliable. Using the reconstruction techniques for the Lagrange multiplier  $F(R)$  gravity, we construct the form of effective  $F(R)$  gravity that can realize such a cosmological evolution, and we determine the power spectrum of the primordial curvature perturbations. Accordingly, we calculate the spectral index of the primordial curvature perturbations and the tensor-to-scalar ratio, and we confront these with the latest observational data. We also address the issue of stability of the primordial metric perturbations, and to this end, we determine the form of  $F(R)$  which realizes the nonsingular cosmology for the whole range of cosmic time  $-\infty < t < \infty$ , by solving the Friedmann equations without the “low-curvature” approximation. This study is performed numerically though, due to the high complexity of the resulting differential equations. By using this numerical solution, we show that the stability is achieved for the same range of values of the free parameters that guarantee the phenomenological viability of the model. We also investigate the energy conditions in the present context. The phenomenology of the no-singular bounce is also studied in the context of a standard  $F(R)$  gravity. We find that the results obtained in the Lagrange multiplier  $F(R)$  gravity model have differences in comparison to the standard  $F(R)$  gravity model, where the observable indices are not simultaneously compatible with the latest Planck results, and also the standard  $F(R)$  gravity model is plagued with instabilities of the perturbation. These facts clearly justify the importance of the Lagrange multiplier field in making the observational indices compatible with the Planck data and also in removing the instabilities of the metric perturbations. Thereby, the bounce with the aforementioned scale factor is adequately described by the Lagrange multiplier  $F(R)$  gravity, in comparison to the standard  $F(R)$  model.

DOI: 10.1103/PhysRevD.100.084056

**I. INTRODUCTION**

According to standard cosmology, the early Universe was dense and hot and it seems that the timelike geodesics have a focal point or a focal bundle, which in most cases is assumed that it leads to the big bang primordial singularity. The big bang singularity is an assumption or a direct consequence of classical equations of motion; however, this singularity

\*nojiri@gravity.phys.nagoya-u.ac.jp

†odintsov@ieec.uab.es

‡v.k.oikonomou1979@gmail.com

§pul.tnmy9@gmail.com

cannot be perceived as a point in spacetime, but as an initial spacelike three dimensional hypersurface, due to the fact that if it was a point, this would lead to infinitely causally disconnected regions in the Universe. Apart from these theoretical conceptual problems, it is known that any singularity in a classical Universe must be dressed inside a horizon. It is possible that the big bang singularity, which is a past spacelike singularity, is just a manifestation of the underlying quantum theory of gravity, as in classical electrodynamics Coulomb potential singularities at the origin of the potential, which are resolved in the context of quantum electrodynamics. Having these in mind, it is apparent that the theories which conceptually lead to a big bang singularity are haunted by the above conceptual problems.

An alternative theory that is free from the above problems is the so-called big bounce theory, or bouncing cosmology in general [1–46]. Bouncing cosmologies are free from primordial initial singularities, since the Universe initially contracts until it reaches a minimal size, and then bounces off at a specific cosmic time instance and starts to expand again. This process can be repeated for an infinite number of times; this is why sometimes bouncing cosmologies are also known as cyclic cosmologies. Bounce cosmology is also appealing since it is derived as a cosmological solution from loop quantum cosmology theory [47–62].

Among various bouncing models proposed over the last several years, the matter bounce scenario [6,15,16,52,62–73] earned special attention, since it can provide a nearly scale invariant power spectrum of primordial curvature perturbations. The matter bounce scenario is essentially characterized by the Universe evolved through a nearly matter dominated epoch at very early times in the contracting phase, in order to obtain an approximately scale invariant power spectrum, and gradually evolves towards a bounce where all the parts of the Universe become in causal contact [74], solving the horizon problem. After it bounces off, it enters a regular expanding phase, in which it matches the behavior of the standard big bang cosmology. However in order to obtain a viable matter bounce scenario, it is expected that the underlying model is consistent with various observational constraints that are put by the latest Planck data. Moreover there are several conceptual issues that are not clear in the framework of matter bounce scenario. First, in an exact matter bounce scenario, materialized by using a single scalar field model, the power spectrum is exactly scale invariant, which is in tension with the observational constraints. The inconsistency of spectral index in the context of matter bounce scenario was also confirmed in [70] from a slightly different point of view. Second, according to the Planck 2018 data, the running of the spectral index is constrained to be  $-0.0085 \pm 0.0073$ . However, for the single scalar field matter bounce scenario model, the running of the index becomes zero and hence does not comply with the observations. At this stage it deserves mentioning that the running of the spectral index

is still not a parameter of the standard model of cosmology. In other words,  $\alpha_s$  is consistent with the value 0. Indeed, one cannot say that  $\alpha_s$  is different than zero by much more than  $1\sigma$ . All this to say that it is a little harsh to confirm that a model does not comply with observations when it is within  $2\sigma$ . At most, predicting  $\alpha_s = 0$  could be in slight tension ( $< 2\sigma$ ) with observations. Predicting running in excess of the measured value (by more than  $2\sigma$  for instance) is a bigger issue. Third, in the simplest model of matter bounce scenario, the amplitude of tensor fluctuation is comparable to that of curvature perturbation and thus the value of tensor-to-scalar ratio is of the order  $\sim \mathcal{O}(1)$ , which is in conflict with the Planck constraints. However, in a quasimatter bounce scenario (instead of an exact matter bounce), according to which the scale factor of the Universe evolves as  $t^{\frac{2}{3(1+w)}}$  (with  $w \neq 0$ ), deeply in the contracting era, it is possible to recover the consistency of spectral index and the running index even in a single scalar field model, but the tensor-to-scalar ratio is still problematic. Moreover, in the context of standard  $F(R)$  gravity, neither matter bounce nor quasimatter bounce are consistent with the Planck data, as we will demonstrate at a later section.

Motivated by the above arguments, we shall consider a variant nonsingular bounce with scale factor  $a(t) = (a_0 t^2 + 1)^n$  in the context of the Lagrange multiplier  $F(R)$  theory of gravity [75] and try to explore whether the matter bounce ( $n = 1/3$ ) or the quasimatter bounce [ $n \sim \mathcal{O}(1/3)$ ] scenario is viable in such a generalized  $F(R)$  gravity [76,77] framework. Our discussions are extended to investigate the stability conditions of the primordial metric perturbations and the energy conditions in the present context. We further study the phenomenology of the aforementioned bouncing model in the context of standard  $F(R)$  gravity. By comparing the results obtained from the Lagrange multiplier  $F(R)$  gravity with that of the standard  $F(R)$  gravity model, we establish the importance of the Lagrange multiplier field from various perspectives.

The paper is organized as follows: In Sec. II, we briefly discuss the generalized  $F(R)$  gravity model in the presence of a Lagrange multiplier term. Sections III, IV, and V are devoted to the explicit calculation of the power spectrum, the observational indices, the stability conditions of the primordial perturbations and the investigation of the energy conditions in the Lagrange multiplier  $F(R)$  gravity model. Section VI is devoted on the realization of the bouncing model under study with standard  $F(R)$  gravity, and its comparison with that of the Lagrange multiplier  $F(R)$  gravity model. The conclusions follow at the end of the paper.

## II. ESSENTIAL FEATURES OF LAGRANGE MULTIPLIER $F(R)$ GRAVITY

Let us briefly recall the formalism of the Lagrange multiplier  $F(R)$  gravity developed in Ref. [75]. The action of the model is

$$S = \frac{1}{2\kappa^2} \int d^4x \sqrt{-g} [F(R) + \lambda(\partial_\mu \Phi \partial^\mu \Phi + G(R))], \quad (1)$$

where  $\kappa^2 = \frac{1}{M^2}$  with  $M$  being the four dimensional Planck mass  $\sim 10^{19}$  GeV. Here,  $F(R)$  and  $G(R)$  are two differentiable functions of the Ricci scalar  $R$ ,  $\Phi$  is a scalar field with a self-coupling kinetic term and the coupling is determined by the function  $\lambda$ , known as the Lagrange multiplier, in the action (1). It was shown in [75] that such variant theory of  $F(R)$  gravity with the Lagrange multiplier term is free of ghosts. The variation of the action with respect to the function  $\lambda$  and with respect to the scalar field  $\Phi$  lead to the following equations of motion:

$$\partial_\mu \Phi \partial^\mu \Phi + G(R) = 0, \quad \nabla_\mu (\lambda \partial^\mu \Phi) = 0. \quad (2)$$

On the other hand, by varying the action with respect to the metric tensor  $g^{\mu\nu}$ , we obtain

$$\begin{aligned} \frac{1}{2} F(R) g_{\mu\nu} - (F'(R) + \lambda G'(R)) R_{\mu\nu} - \lambda \partial_\mu \Phi \partial_\nu \Phi \\ + (\nabla_\mu \nabla_\nu - g_{\mu\nu} \nabla^2)(F'(R) + \lambda G'(R)) = 0. \end{aligned} \quad (3)$$

As we are interested in cosmological scenario in the present context, we shall assume that the background geometry is described by a flat Friedman-Robertson-Walker (FRW) metric,

$$ds^2 = -dt^2 + a(t)^2(dx^2 + dy^2 + dz^2), \quad (4)$$

where  $a(t)$  is the scale factor of the Universe. As it is evident from Eq. (4), the Universe is considered to be homogeneous and isotropic and thus the function  $\lambda$  and the scalar field are taken as functions of the cosmic time  $t$ . In effect of the metric given in Eq. (4), the field equations in (2) take the following form:

$$-\dot{\Phi}^2 + G(R) = 0, \quad \frac{d}{dt}(a^3 \lambda \dot{\Phi}) = 0, \quad (5)$$

which can be solved as

$$\dot{\Phi} = \sqrt{G(R)}, \quad a^3 \lambda \dot{\Phi} = E, \quad (6)$$

with  $E$  being a constant of the integration. Using these solutions along with the FRW metric, we obtain the temporal and spatial component of Eq. (3) as follows:

$$\begin{aligned} -\frac{F(R)}{2} + 3(\dot{H} + H^2) \left( F'(R) + \frac{EG'}{a^3 \sqrt{G}} \right) - \frac{E\sqrt{G}}{a^3} \\ - 3H \frac{d}{dt} \left( F'(R) + \frac{EG'}{a^3 \sqrt{G}} \right) = 0, \end{aligned} \quad (7)$$

and

$$\begin{aligned} \frac{F(R)}{2} - (\dot{H} + 3H^2) \left( F'(R) + \frac{EG'}{a^3 \sqrt{G}} \right) \\ + \left( \frac{d^2}{dt^2} + 2H \frac{d}{dt} \right) \left( F'(R) + \frac{EG'}{a^3 \sqrt{G}} \right) = 0, \end{aligned} \quad (8)$$

respectively, where  $H(t) = \frac{\dot{a}}{a}$  is the Hubble rate. It may be noticed that for  $E = 0$ , the gravitational equations become identical with those of standard  $F(R)$  gravity. Having the equations at hand, our next task is to reconstruct the forms of  $F(R)$  and  $G(R)$  that can realize a bouncing cosmology of specific form, which is the subject of the next section.

### III. REALIZATION OF BOUNCING COSMOLOGY

In the present section, we shall investigate which functional forms of  $F(R)$  and  $G(R)$  can realize a bouncing Universe cosmological scenario, with the following scale factor:

$$a(t) = (a_0 t^2 + 1)^n, \quad (9)$$

where  $a_0$  and  $n$  are the model free parameters, with  $a_0$  having mass dimension [+2], while  $n$  is dimensionless. The Universe's evolution in a general bouncing cosmology, consists of two eras: an era of contraction and an era of expansion. It is obvious that the above scale factor describes a contracting era for the Universe, when  $t \rightarrow -\infty$ , then the Universe reaches a bouncing point at  $t = 0$  at which the Universe has a minimal size, and then the Universe starts to expand again, for cosmic times  $t > 0$ . Hence, the Universe in this scenario never develops a crushing type big bang singularity. It may be mentioned that for  $n = 1/3$ , the scale factor describes the matter bounce scenario. Equation (9) leads to the following Hubble rate and its first derivative:

$$H(t) = \frac{2nt}{t^2 + 1/a_0}, \quad \dot{H}(t) = -2n \frac{t^2 - 1/a_0}{(t^2 + 1/a_0)^2}. \quad (10)$$

With the help of the above expressions, the Ricci scalar is found to be

$$R(t) = 12H^2 + 6\dot{H} = 12n \left[ \frac{(4n-1)t^2 + 1/a_0}{(t^2 + 1/a_0)^2} \right]. \quad (11)$$

Using Eq. (11), one can determine the cosmic time as a function of the Ricci scalar, that is the function  $t = t(R)$ . As a result, the Hubble rate and its first derivative can be expressed in terms of  $R$  (however this statement holds for all analytic functions of  $t$ ) and also the differential operator  $\frac{d}{dt}$  can be written as  $\frac{d}{dt} = \dot{R}(R) \frac{d}{dR}$ . By plugging the resulting expressions in Eqs. (7) and (8), we obtain differential equations which determine the functional form of  $F(R)$ ,  $G(R)$  fully in terms of  $R$ , and by solving those differential equations, the forms of  $F(R)$  and  $G(R)$  can be found.

However the differential equations will become cumbersome to provide analytic solutions and thus we consider the low-curvature limit of the theory, that is,  $\frac{R}{a_0} \ll 1$  for the purpose of reconstruction. This approximation will prove to be quite useful since as we show in a later section, the primordial perturbations of the matter bounce scenario are generated deeply in the contraction era, at  $t \rightarrow -\infty$  ( $t^2 \gg 1/a_0$ ), in which case  $H \ll \sqrt{a_0}$  and therefore the curvature is quite small ( $\frac{R}{a_0} \ll 1$ ).

During the low-curvature regime (or at large negative time),  $R(t)$  can be written as  $R(t) \sim \frac{12n(4n-1)}{t^2}$  from Eq. (11). This helps to express the scale factor, the Hubble rate, its first derivative, and the differential operators  $d/dt$ ,  $d^2/dt^2$ , in terms of the Ricci scalar  $R$  as follows:

$$a(R) = \frac{[12na_0^n(4n-1)]^n}{R^n}, \quad H(R) = 2n\sqrt{\frac{R}{12n(4n-1)}},$$

$$\dot{H}(R) = -2n\sqrt{\frac{R}{12n(4n-1)}}, \quad (12)$$

and

$$\frac{d}{dt} = -24n(4n-1) \left[ \frac{R}{12n(4n-1)} \right]^{3/2} \frac{d}{dR},$$

$$\frac{d^2}{dt^2} = \frac{1}{3n(4n-1)} \left[ R^3 \frac{d^2}{dR^2} + \frac{3}{2} R^2 \frac{d}{dR} \right], \quad (13)$$

respectively. By plugging back these expressions to Eqs. (7) and (8), and by introducing  $J(R) = F(R) + \frac{2E\sqrt{G(R)}}{a^3(R)}$ , we get the following differential equations:

$$\frac{2}{(4n-1)} R^2 \frac{d^2 J}{dR^2} - \frac{(1-2n)}{(4n-1)} R \frac{dJ}{dR} - J(R) = 0, \quad (14)$$

and

$$F(R) = \frac{(6n-1)}{3n(4n-1)} R \frac{dJ}{dR} - \frac{(3-4n)}{3n(4n-1)} R^2 \frac{d^2 J}{dR^2}$$

$$- \frac{2}{3n(4n-1)} R^3 \frac{d^3 J}{dR^3}. \quad (15)$$

Equation (14) has the following solution:

$$J(R) = AR^\rho + BR^\delta, \quad (16)$$

where  $\rho = \frac{1}{4}[3-2n-\sqrt{1+4n(5+n)}]$  and  $\delta = \frac{1}{4}[3-2n+\sqrt{1+4n(5+n)}]$  and also  $A$  and  $B$  are integration constants having mass dimension  $[2-2\rho]$  and  $[2-2\delta]$ , respectively. This solution of  $J(R)$  along with Eq. (15) lead to the following functional form of  $F(R)$ :

$$F(R) = A \left[ \frac{(6n-1)}{3n(4n-1)} \rho - \frac{(3-4n)}{3n(4n-1)} \rho(\rho-1) \right. \\ \left. - \frac{2}{3n(4n-1)} \rho(\rho-1)(\rho-2) \right] R^\rho \\ + B \left[ \frac{(6n-1)}{3n(4n-1)} \delta - \frac{(3-4n)}{3n(4n-1)} \delta(\delta-1) \right. \\ \left. - \frac{2}{3n(4n-1)} \delta(\delta-1)(\delta-2) \right] R^\delta \\ = CR^\rho + DR^\delta, \quad (17)$$

where  $C$  and  $D$  are the corresponding coefficients of  $R^\rho$  and  $R^\delta$ , respectively. With these solutions, the effective  $f(R)$  can be written as

$$f(R) = F(R) + \lambda G(R) = \frac{1}{2} [J(R) + F(R)] \\ = \frac{1}{2} (A+C)R^\rho + \frac{1}{2} (B+D)R^\delta \quad (18)$$

where we use the solution of  $\lambda(t) = \frac{E}{a^3\sqrt{G}}$ . Thus Eqs. (16), (17), and (18) are the main results of the present section. In the next section we address concretely the cosmological perturbations issue and we shall confront the theory with the observational data.

#### IV. COSMOLOGICAL PERTURBATION: OBSERVABLE QUANTITIES AND THE STABILITY CONDITION

In this section we shall study the first order metric perturbations of the theory at hand, following Refs. [78–80], where the scalar and tensor perturbations are calculated for various variants of higher curvature gravity models. Scalar, vector, and tensor perturbations are decoupled, as in general relativity, so that we can focus our attention on tensor and scalar perturbations separately.

##### A. Scalar perturbations

The scalar perturbation of FRW background metric is defined as follows:

$$ds^2 = -(1+2\Psi)dt^2 + a(t)^2(1-2\Psi)\delta_{ij}dx^i dx^j, \quad (19)$$

where  $\Psi(t, \vec{x})$  denotes the scalar perturbation. In principle, perturbations should always be expressed in terms of gauge invariant quantities, in our case the comoving curvature perturbation defined as  $\mathfrak{R} = \Psi - aHv$ , where  $v(t, \vec{x})$  is the velocity perturbation. However, we shall work in the comoving gauge condition, where the velocity perturbation is taken as zero, thus with such gauge fixing  $\mathfrak{R} = \Psi$ . Thereby, we can work with the perturbed variable  $\Psi(t, \vec{x})$ . The perturbed action up to  $\Psi^2$  order is [78]

$$\delta S_\psi = \int dt d^3\vec{x} a(t) z(t)^2 \left[ \dot{\Psi}^2 - \frac{1}{a^2} (\partial_i \Psi)^2 \right], \quad (20)$$

where  $z(t)$  has the following expression:

$$z(t) = \frac{a(t)}{\left( H(t) + \frac{1}{2f'(R)} \frac{df'(R)}{dt} \right)} \sqrt{\frac{2E\sqrt{G}}{a^3} + \frac{3}{2f'(R)} \left( \frac{df'(R)}{dt} \right)^2}. \quad (21)$$

It is evident from Eq. (20), that  $c_s^2 = 1$ , which guarantees the absence of ghost modes or equivalently one may argue that the model is free from gradient instability. Also stability of the scalar perturbations is ensured if  $z(t)^2 > 0$ . This stability issue must be checked for all cosmic times, including the bouncing point, in which case the low-curvature approximation does not hold true anymore, and it will be thoroughly studied at a later section. Specifically, we will examine the stability of perturbation by reconstructing  $F(R)$  and  $G(R)$  beyond the low-curvature limit, numerically, due to the complexity of the resulting differential equations when the low-curvature approximation does not hold true anymore.

However at present, we concentrate on determining various observable quantities and specifically, the spectral index of the primordial curvature perturbations, the tensor-to-scalar ratio, and the running of the spectral index, which are eventually determined at the time of horizon exit. For the scale factor we consider in the present paper, the horizon exit occurs during the low-curvature regime deeply in the contracting era. Thereby, for the purpose of finding the observable parameters, the condition  $R/a_0 \ll 1$  stands as a viable approximation.

In the low-curvature limit, we determine various terms present in the expression of  $z(t)$  [see Eq. (21)] as

$$\begin{aligned} & \frac{a(t)}{\left( H(t) + \frac{1}{2f'(R)} \frac{df'(R)}{dt} \right)} \\ &= \frac{a_0^n (12n(4n-1))^{n+1/2}}{R^{n+1/2}} \\ & \times \left[ 2n - \frac{(\rho-1) \left[ 1 + \frac{\delta(\delta-1)(B+D)}{\rho(\rho-1)(A+C)} R^{\delta-\rho} \right]}{\left[ 1 + \frac{\delta(B+D)}{\rho(A+C)} R^{\delta-\rho} \right]} \right]^{-1}, \end{aligned}$$

and

$$\begin{aligned} & \frac{2E\sqrt{G}}{a^3} + \frac{3}{2f'(R)} \left( \frac{df'(R)}{dt} \right)^2 \\ &= R^\rho \left[ (A-C) \left( 1 + \frac{(B-D)}{(A-C)} R^{\delta-\rho} \right) \right. \\ & \left. + \frac{\rho(A+C)(\rho-1)^2 \left[ 1 + \frac{\delta(\delta-1)(B+D)}{\rho(\rho-1)(A+C)} R^{\delta-\rho} \right]^2}{4n(4n-1) \left[ 1 + \frac{\delta(B+D)}{\rho(A+C)} R^{\delta-\rho} \right]} \right]. \end{aligned}$$

Consequently  $z(t)$  takes the following form:

$$z(t) = \sqrt{3} a_0^n [12n(4n-1)]^n \frac{\sqrt{P(R)}}{Q(R)} \frac{1}{R^{n+1/2-\rho/2}}, \quad (22)$$

where  $P(R)$  and  $Q(R)$  are defined as follows:

$$P(R) = \left[ 4n(4n-1)(A-C) \left( 1 + \frac{(B-D)}{(A-C)} R^{\delta-\rho} \right) + \frac{\rho(A+C)(\rho-1)^2 \left[ 1 + \frac{\delta(\delta-1)(B+D)}{\rho(\rho-1)(A+C)} R^{\delta-\rho} \right]^2}{\left[ 1 + \frac{\delta(B+D)}{\rho(A+C)} R^{\delta-\rho} \right]} \right], \quad (23)$$

and

$$Q(R) = \left[ 2n - \frac{(\rho-1) \left[ 1 + \frac{\delta(\delta-1)(B+D)}{\rho(\rho-1)(A+C)} R^{\delta-\rho} \right]}{\left[ 1 + \frac{\delta(B+D)}{\rho(A+C)} R^{\delta-\rho} \right]} \right]. \quad (24)$$

Before moving further, at this stage, we check whether  $Q(R)$  goes to zero or equivalently  $z(t) \rightarrow \infty$  at some point in time. This issue is known to occur in Horndeski theories; see for example [81–83]. It is important to examine because as we will show, the Mukhanov-Sasaki equation (which is essential to determine the observable quantities) has a term containing  $1/z(t)$  and moreover the Mukhanov variable ( $v = z\Psi$ ) diverges at the point when  $z(t)$  goes to infinity. As mentioned earlier, the perturbations generate in the low curvature regime deeply in the contracting era and thus the above expression of  $Q$  can be simplified as follows:

$$Q(R) = (2n - \rho + 1) - \frac{\delta(\delta - \rho)(B + D)}{\rho(A + C)} R^{\delta - \rho} \quad (25)$$

where  $\rho = \frac{1}{4}[3 - 2n - \sqrt{1 + 4n(5 + n)}]$ ,  $\delta = \frac{1}{4}[3 - 2n + \sqrt{1 + 4n(5 + n)}]$ , and  $A, B$  are two integration constants. Further, recall, the explicit expressions of  $C$  and  $D$  [see Eq. (17)] are given by

$$\begin{aligned} C &= A \left[ \frac{(6n-1)}{3n(4n-1)} \rho - \frac{(3-4n)}{3n(4n-1)} \rho(\rho-1) \right. \\ & \quad \left. - \frac{2}{3n(4n-1)} \rho(\rho-1)(\rho-2) \right] \\ D &= B \left[ \frac{(6n-1)}{3n(4n-1)} \delta - \frac{(3-4n)}{3n(4n-1)} \delta(\delta-1) \right. \\ & \quad \left. - \frac{2}{3n(4n-1)} \delta(\delta-1)(\delta-2) \right] \end{aligned}$$

Putting these expressions of  $C$  and  $D$  into Eq. (25) we get

$$Q(R) = (2n - \rho + 1) - \frac{B\delta(\delta - \rho)\left(1 + \frac{(6n-1)}{3n(4n-1)}\delta - \frac{(3-4n)}{3n(4n-1)}\delta(\delta - 1) - \frac{2}{3n(4n-1)}\delta(\delta - 1)(\delta - 2)\right)}{A\rho\left(1 + \frac{(6n-1)}{3n(4n-1)}\rho - \frac{(3-4n)}{3n(4n-1)}\rho(\rho - 1) - \frac{2}{3n(4n-1)}\rho(\rho - 1)(\rho - 2)\right)} R^{\delta-\rho}. \quad (26)$$

Using the forms of  $\rho$  and  $\delta$  (in terms of  $n$ ), it can be checked that the above expression of  $Q$  is a positive definite quantity (or does not hit to the value zero) for  $n > \frac{1}{4}$ . Moreover we will show in the later sections that the observable quantities are compatible with Planck observations for the parametric regime  $0.27 \lesssim n \lesssim 0.40$  (i.e., for  $n > 1/4$ ). Therefore  $Q(t)$  does not hit to zero or equivalently  $z(t)$  does not tend to infinity for the parametric values which are consistent with the Planck observations. It may be mentioned that such nondivergent character of  $z(t)$  has been investigated here in the low curvature regime (or at large negative time where the perturbation modes are generated). Thus there remains the possibility that  $z(t)$  goes to infinity in the large curvature regime near the bounce phase; however, this may not be a physical issue and may be resolved by studying the perturbations near this singularity in the perturbation equations in another gauge.

Equation (20) clearly indicates that  $\Psi(t, \vec{x})$  is not canonically normalized and to this end we introduce the well-known Mukhanov-Sasaki variable as  $v = z\Psi$  (as we are working in the comoving gauge). The corresponding fourier mode of the Mukhanov-Sasaki variable satisfies

$$\frac{d^2 v_k}{d\tau^2} + \left(k^2 - \frac{1}{z(\tau)} \frac{d^2 z}{d\tau^2}\right) v_k(\tau) = 0, \quad (27)$$

$$\frac{1}{z} \frac{d^2 z}{d\tau^2} = \frac{\xi(\xi - 1)}{\tau^2} \left[ 1 + \frac{2(\delta - \rho)}{(\xi - 1)} R^{\delta-\rho} \left( \frac{\delta(\rho - \delta)(B + D)}{\rho(A + C)(2n - \rho + 1)} + \frac{\delta(1 - \rho)(1 + \rho - 2\delta)(B + D) + 4(B - D)n + 16(B - D)n^2}{\rho(1 - \rho)^2(A + C) + 4(A - C)n + 16(A - C)n^2} \right) \right], \quad (30)$$

with  $\xi = \frac{(2n+1-\rho)}{(1-2n)}$ . Recall  $\rho = \frac{1}{4}[3 - 2n - \sqrt{1 + 4n(5 + n)}]$  and  $\delta = \frac{1}{4}[3 - 2n + \sqrt{1 + 4n(5 + n)}]$ , which clearly indicate that  $\delta - \rho$  is a positive quantity. Thus the term within parentheses in Eq. (30) can be safely considered to be small in the low-curvature regime  $R/a_0 \ll 1$ . As a result,  $\frac{1}{z} \frac{d^2 z}{d\tau^2}$  becomes proportional to  $1/\tau^2$  i.e.,  $\frac{1}{z} \frac{d^2 z}{d\tau^2} = \sigma/\tau^2$  with

$$\sigma = \xi(\xi - 1) \left[ 1 + \frac{2(\delta - \rho)}{(r - 1)} R^{\delta-\rho} \left( \frac{\delta(\rho - \delta)(B + D)}{\rho(A + C)(2n - \rho + 1)} + \frac{\delta(1 - \rho)(1 + \rho - 2\delta)(B + D) + 4(B - D)n + 16(B - D)n^2}{\rho(1 - \rho)^2(A + C) + 4(A - C)n + 16(A - C)n^2} \right) \right], \quad (31)$$

which is approximately a constant in the era, when the primordial perturbation modes generate deep inside the Hubble radius. In effect, and in conjunction with the fact that  $c_s^2 = 1$ , the Mukhanov equation can be solved as follows:

$$v(k, \tau) = \frac{\sqrt{\pi|\tau|}}{2} [c_1(k)H_\nu^{(1)}(k|\tau|) + c_2(k)H_\nu^{(2)}(k|\tau|)], \quad (32)$$

where  $\tau = \int dt/a(t)$  is the conformal time and  $v_k(\tau)$  is the Fourier transformed variable of  $v(t, \vec{x})$  for the  $k$ th mode. Equation (27) is quite difficult to solve analytically in general, since the function  $z$  depends on the background dynamics. However the equation can be solved analytically in the regime  $R/a_0 \ll 1$  as we now show. The conformal time ( $\tau$ ) is related to the cosmic time ( $t$ ) as  $\tau = \int \frac{dt}{a(t)} = \frac{1}{a_0^{n(1-2n)}} t^{1-2n}$  for  $n \neq 1/2$ ; however, we will show that the observable quantities are compatible with Planck data [84] for  $n < 1/2$  and thus we can safely work with the aforementioned expression of  $\tau = \tau(t)$ . Using this, we can express the Ricci scalar as a function of the conformal time,

$$R(\tau) = \frac{12n(4n - 1)}{\tau^2} = \frac{12n(4n - 1)}{[a_0^n(1 - 2n)]^{2/(1-2n)} \tau^{2/(1-2n)}}. \quad (28)$$

Having this in mind, along with Eq. (22), we can express  $z$  in terms of  $\tau$  as follows:

$$z(\tau) = \sqrt{3}a_0^n [12n(4n - 1)]^n \frac{\sqrt{P(\tau)}}{Q(\tau)} \tau^{\frac{2n+1-\rho}{1-2n}}. \quad (29)$$

The above expression of  $z = z(\tau)$  yields the expression of  $\frac{1}{z} \frac{d^2 z}{d\tau^2}$ , which is essential for the Mukhanov equation,

with  $\nu = \sqrt{\sigma + \frac{1}{4}}$  and  $c_1$  and  $c_2$  are integration constants. Assuming the Bunch-Davies vacuum initially, these integration constants become  $c_1 = 0$  and  $c_2 = 1$ , respectively. Having the solution of  $v_k(\tau)$  at hand, next we proceed to evaluate the power spectrum (defined for the Bunch-Davies vacuum state) corresponding to the  $k$ th scalar perturbation mode, which is defined as follows:

$$P_{\Psi}(k, \tau) = \frac{k^3}{2\pi^2} |\Psi_k(\tau)|^2 = \frac{k^3}{2\pi^2} \left| \frac{v_k(\tau)}{z(\tau)} \right|^2. \quad (33)$$

In the superhorizon limit, using the mode solution in Eq. (32), we have

$$P_{\Psi}(k, \tau) = \left[ \frac{1}{2\pi} \frac{1}{z|\tau|} \frac{\Gamma(\nu)}{\Gamma(3/2)} \right]^2 \left( \frac{k|\tau|}{2} \right)^{3-2\nu}. \quad (34)$$

By using Eq. (34), we can determine the observable quantities like spectral index of the primordial curvature perturbations and the running of spectral index. Before proceeding to calculate these observable quantities, we will consider first the tensor power spectrum, which is necessary for evaluating the tensor-to-scalar ratio.

### B. Tensor perturbations

Let us now focus on the tensor perturbations, and the tensor perturbation on the FRW metric background is defined as follows:

$$ds^2 = -dt^2 + a(t)^2(\delta_{ij} + h_{ij})dx^i dx^j, \quad (35)$$

where  $h_{ij}(t, \vec{x})$  is the tensor perturbation. The tensor perturbation is itself a gauge invariant quantity, and the tensor perturbed action up to quadratic order is given by

$$\delta S_h = \int dt d^3\vec{x} a(t) z_T(t)^2 \left[ \dot{h}_{ij} \dot{h}^{ij} - \frac{1}{a^2} (\partial_k h_{ij})^2 \right], \quad (36)$$

where  $z_T(t)$  is given by

$$z_T(t) = a \sqrt{f'(R)}. \quad (37)$$

Therefore, the speed of the tensor perturbation propagation is  $c_T^2 = 1$ . Moreover the tensor perturbation is stable if the condition  $z_T^2 > 0$  is satisfied, and in a later section we shall examine in detail whether this condition is satisfied.

Similar to scalar perturbation, the Mukhanov-Sasaki variable for tensor perturbation is defined as  $(v_T)_{ij} = z_T h_{ij}$  which, upon performing the Fourier transformation, satisfies the following equation:

$$\frac{d^2 v_T(k, \tau)}{d\tau^2} + \left( k^2 - \frac{1}{z_T(\tau)} \frac{d^2 z_T}{d\tau^2} \right) v_T(k, \tau) = 0. \quad (38)$$

By using Eq. (37), along with the condition  $R/a_0 \ll 1$ , we evaluate  $z_T(\tau)$  and  $\frac{1}{z_T(\tau)} \frac{d^2 z_T}{d\tau^2}$  and these read

$$z_T(\tau) = a_0^n [12n(4n-1)]^n S(\tau) \tau^{\frac{2n+1-\rho}{1-2n}} \quad (39)$$

and

$$\frac{1}{z_T} \frac{d^2 z_T}{d\tau^2} = \frac{\xi(\xi-1)}{\tau^2} \left[ 1 - \frac{2\delta(\delta-\rho)(B+D)}{(r-1)\rho(A+C)} R^{\delta-\rho} \right], \quad (40)$$

respectively, where  $S(R(\tau)) = \sqrt{\frac{\rho(A+C)}{2}} \left[ 1 + \frac{\delta(B+D)}{\rho(A+C)} R^{\delta-\rho} \right]^{1/2}$  and also we use  $R = R(\tau)$  from Eq. (28). Due to the fact that  $\delta-\rho$  is positive, the variation of the term in the parentheses in Eq. (40) can be regarded to be small in the low-curvature regime and thus  $\frac{1}{z_T} \frac{d^2 z_T}{d\tau^2}$  becomes proportional to  $1/\tau^2$ , that is  $\frac{1}{z_T} \frac{d^2 z_T}{d\tau^2} = \sigma_T/\tau^2$ , with

$$\sigma_T = \xi(\xi-1) \left[ 1 - \frac{2\delta(\delta-\rho)(B+D)}{(r-1)\rho(A+C)} R^{\delta-\rho} \right], \quad (41)$$

and recall  $\xi = \frac{(2n+1-\rho)}{(1-2n)}$ . The above expressions yield the tensor power spectrum, defined with initial state the Bunch-Davies vacuum, so we have

$$P_h(k, \tau) = 2 \left[ \frac{1}{2\pi} \frac{1}{z_T|\tau|} \frac{\Gamma(\nu_T)}{\Gamma(3/2)} \right]^2 \left( \frac{k|\tau|}{2} \right)^{3-2\nu_T}. \quad (42)$$

The factor 2 arises due to the two polarization modes of the gravity wave, and  $\nu_T = \sqrt{\sigma_T + \frac{1}{4}}$  where  $\sigma_T$  is defined in Eq. (41).

Now we can explicitly confront the model at hand with the latest Planck observational data [84], so we shall calculate the spectral index of the primordial curvature perturbations  $n_s$  and the tensor-to-scalar ratio  $r$ , which are defined as follows:

$$n_s = 1 + \frac{\partial \ln P_{\Psi}}{\partial \ln k} \Big|_{\tau=\tau_h}, \quad r = \frac{P_h(k, \tau)}{P_{\Psi}(k, \tau)} \Big|_{\tau=\tau_h}. \quad (43)$$

Equations (34) and (42) immediately lead to the explicitly form of  $n_s$  and  $r$  as follows:

$$n_s = 4 - \sqrt{1 + 4\sigma}, \quad r = 2 \left[ \frac{z(\tau)}{z_T(\tau)} \right]_{\tau=\tau_h}^2, \quad (44)$$

where  $\sigma$ ,  $z(\tau)$ , and  $z_T(\tau)$  are given in Eqs. (31), (28), and (39), respectively. As it is evident from the above equations,  $n_s$  and  $r$  are evaluated at the time of horizon exit, when  $k = aH$ , or equivalently at  $\tau = \tau_h$ . It may be noticed that  $n_s$  and  $r$  depend on the dimensionless parameters  $\frac{R_h}{a_0}$  and  $n$  with  $R_h = R(\tau_h)$ . We can now directly confront the spectral index and the tensor-to-scalar ratio with the Planck 2018 constraints [84], which constrain the observational indices as follows:

$$n_s = 0.9649 \pm 0.0042, \quad r < 0.064. \quad (45)$$

For the model at hand,  $n_s$  and  $r$  are within the Planck constraints for the following ranges of parameter values:  $0.01 \leq \frac{R_h}{a_0} \leq 0.07$  and  $0.27 \lesssim n \lesssim 0.40$  and this behavior is depicted in Fig. 1. The viable range of  $R_h/a_0$  is in

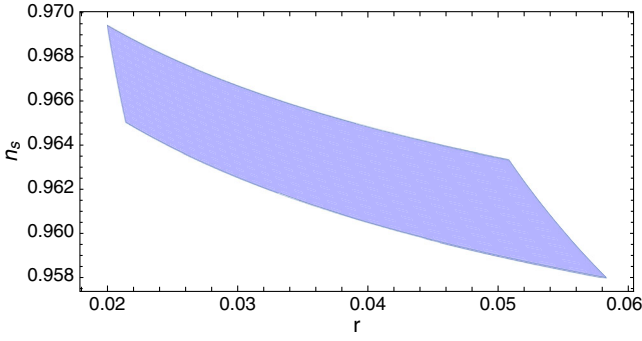


FIG. 1. Parametric plot of  $n_s$  vs  $r$  for  $0.01 \leq \frac{R_h}{a_0} \leq 0.07$  and  $0.27 \lesssim n \lesssim 0.40$ .

agreement with the low-curvature condition  $R/a_0 \ll 1$  that we have considered in our calculations. Moreover the range of the parameter  $n$  clearly indicates that the matter bounce scenario, for which  $n = 1/3$ , is well described by the generalized  $F(R)$  gravity model with the Lagrange multiplier term. At this stage it is worth mentioning that in scalar-tensor theory (with an exponential scalar potential), the matter bounce scenario is not consistent with the Planck observations. Moreover the matter bounce scenario also does not fit well even in the standard  $F(R)$  gravity, as we also confirm in a later section. However, here we show that in the presence of the Lagrange multiplier generalized  $F(R)$  gravity, the matter bounce may be considered as a good bouncing model, which allows the simultaneous compatibility of  $n_s$  and  $r$  with observations.

The results seem to indicate that  $r$  can be suppressed below the current observational bound. One can attribute this to the fact that either scalar fluctuations have been enhanced or that tensor fluctuations have been suppressed in comparison to the “standard” model with Einstein gravity and matter contraction. So, we want to explore which effect comes into play. For Einstein gravity with a scalar field, the gravitational equations of motion turn out to be

$$\begin{aligned} H^2 &= \frac{1}{3} \left[ \frac{1}{2} \dot{\Phi}^2 + V(\Phi) \right], \\ 2\dot{H} + 3H^2 + \frac{1}{2} \dot{\Phi}^2 - V(\Phi) &= 0. \end{aligned} \quad (46)$$

Considering the scale factor  $a(t) = (a_0 t^2 + 1)^n$  along with the help of the above equations of motion, we get the scalar field dynamics and the Ricci scalar as follows:

$$\begin{aligned} \dot{\Phi}(t) &= \frac{2\sqrt{n}}{t}, \\ R(t) &= \frac{12n(4n-1)}{t^2}. \end{aligned} \quad (47)$$

The above solutions are valid under the approximation  $t^2 \gg 1/a_0$  which is a valid one as the perturbations generate at large negative time deeply in the contracting

era. Using the form of the scale factor, we obtain the conformal time in terms of the cosmic time as  $\tau \propto t^{1-2n}$ . These expressions lead to the power spectrum for scalar and tensor perturbations in the case of the standard model of Einstein gravity with matter contraction as follows:

$$\bar{P}_\Psi(k, \tau) = \left[ \frac{1}{2\pi} \frac{1}{\bar{z}|\tau|} \frac{\Gamma(\bar{\nu})}{\Gamma(3/2)} \right]^2 \left( \frac{k|\tau|}{2} \right)^{3-2\bar{\nu}}. \quad (48)$$

and

$$\bar{P}_h(k, \tau) = \frac{2}{M_{\text{pl}}^2} \left[ \frac{1}{2\pi} \frac{1}{\bar{z}_T|\tau|} \frac{\Gamma(\bar{\nu}_T)}{\Gamma(3/2)} \right]^2 \left( \frac{k|\tau|}{2} \right)^{3-2\bar{\nu}_T}, \quad (49)$$

respectively, where the quantities with bar denote the respective quantities in Einstein gravity and  $M_{\text{pl}}$  is the Planck mass. Moreover the explicit expressions of the barred quantities are the following:

$$\begin{aligned} \bar{z} &= \frac{a(t)\dot{\Phi}}{H} \Big|_{t_h} = \frac{[12n(4n-1)]^n}{\sqrt{n}} \left( \frac{a_0}{R_h} \right)^n, \\ \bar{z}_T &= \frac{a(t)}{2} \Big|_{t_h} = \frac{1}{2} [12n(4n-1)]^n \left( \frac{a_0}{R_h} \right)^n, \\ \bar{\nu} &= \bar{\nu}_T = \sqrt{\frac{2n(4n-1)}{(1-2n)^2} + \frac{1}{4}}, \end{aligned} \quad (50)$$

where  $t_h$  is the horizon crossing time,  $R(t_h) = R_h$ , and the factor of  $1/2$  in the expression of  $\bar{z}_T$  ensures that the perturbed action for tensor modes is truly canonically normalized when written in terms of the Mukhanov variable. Therefore it is clear that for matter or quasimatter bounce in Einstein gravity, the scalar and tensor power spectrums are comparable to each other and thus the tensor to scalar ratio ( $r = \frac{\bar{P}_h}{\bar{P}_\Psi}$ ) becomes of the order unity. However in the Lagrange multiplier  $F(R)$  gravity model, the tensor to scalar ratio gets suppressed and matches with the Planck constraints even for matter or quasimatter bounce (as we showed earlier). In order to compare the perturbations of Lagrange multiplier  $F(R)$  gravity model with that of the standard model of Einstein gravity, we give plots of the ratio of the respective power spectrums i.e.,  $P_h/\bar{P}_h$  and  $P_\Psi/\bar{P}_\Psi$  in terms of the parameter  $R_h/a_0$  with  $n = 1/3$  (see Fig. 2). To obtain the plots, we use the horizon crossing relation  $k = aH$ . Figure 2 clearly demonstrates that the tensor power spectrum gets suppressed in the Lagrange multiplier  $F(R)$  model in comparison to Einstein gravity, while the scalar power spectrums remain of same order in both the aforementioned models. This leads to a suppressed tensor-to-scalar ratio in the Lagrange multiplier  $F(R)$  gravity with respect to the standard Einstein model. However the presence of a Lagrange multiplier term may also effect the production of non-Gaussianities, as is also known for  $k$ -essence theories [85] and Horndeski theories [86]. We hope to address this issue in a future work.

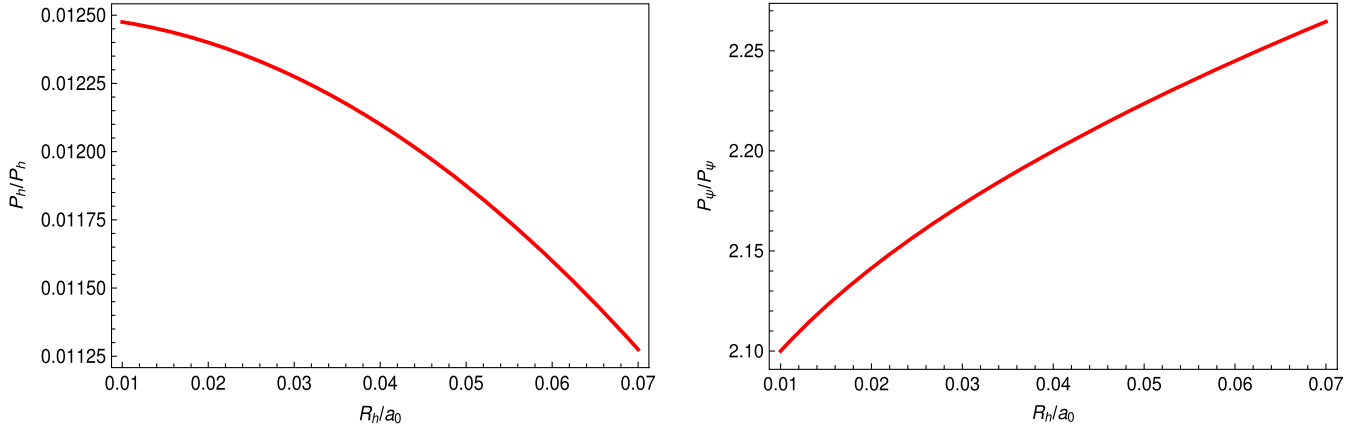


FIG. 2. Left:  $P_h/\bar{P}_h$  vs  $R_h/a_0$  for the purpose of weak energy condition. Right:  $P_\Psi/\bar{P}_\Psi$  vs  $R_h/a_0$  with  $n = 1/3$ .

Furthermore, the running of the spectral index is defined as follows:

$$\alpha = \left. \frac{dn_s}{d \ln k} \right|_{\tau=\tau_h}, \quad (51)$$

and this is constrained by Planck 2018 results as  $\alpha = -0.0085 \pm 0.0073$ . Thus, it is also important to calculate the running of spectral index before concluding the viability of a model. By using the expression of  $\sigma$  [see Eq. (31)] and  $R = R(\tau)$  [see Eq. (28)], we get

$$\alpha = \frac{4\xi(\delta-\rho)^2}{\sqrt{1+4\xi(\xi-1)}} R_h^{\delta-\rho} \left( \frac{\delta(\rho-\delta)(B+D)}{\rho(A+C)(2n-\rho+1)} + \frac{\delta(1-\rho)(1+\rho-2\delta)(B+D) + 4(B-D)n + 16(B-D)n^2}{\rho(1-\rho)^2(A+C) + 4(A-C)n + 16(A-C)n^2} \right). \quad (52)$$

To arrive at the above result, we use the horizon crossing relation of  $k$ th mode  $k = aH$  to determine  $\frac{d|\tau|}{d \ln k} = -|\tau|$  i.e., the horizon exit time  $|\tau|$  increases as the momentum of the perturbation mode decreases, as expected. Equation (52) indicates that as similar to  $n_s$  and  $r$ , the running index ( $\alpha$ ) also depends on the parameters  $R_h/a_0$  and  $n$ . Taking  $R_h/a_0 = 0.05$ , we give a plot of  $\alpha$  with respect to  $n$  in Fig. 3. As it can be seen in Fig. 3, the parameter  $\alpha$  takes negative values, crossing zero near about  $n \simeq 0.30$ . Thus  $\alpha$  lies within the Planck constraint for  $0.30 \lesssim n \lesssim 0.40$ , which includes the matter bounce scenario. For the Lagrange multiplier generalized  $F(R)$  gravity model, we showed that

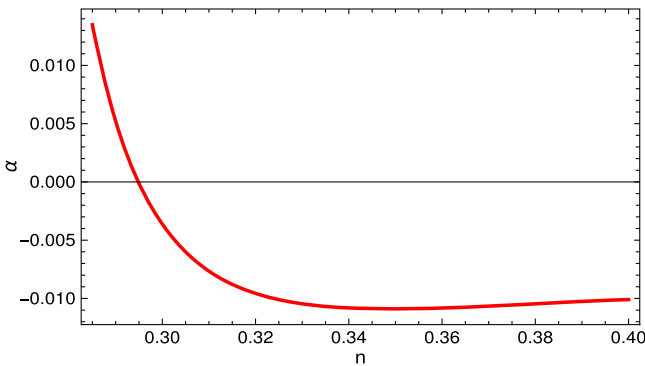


FIG. 3. Parametric plot of  $\alpha$  vs  $n$  for  $\frac{R_h}{a_0} = 0.05$  and  $0.26 \lesssim n \lesssim 0.40$ .

the pure matter bounce scenario as well as the quasimatter bounce scenario are consistent with Planck observations. Therefore the generalized  $F(R)$  gravity with the Lagrange multiplier has a richer phenomenology in comparison to scalar-tensor or standard  $F(R)$  gravity model, which fails to describe in a viable way these two bouncing cosmology scenarios.

### C. Stability of the scalar and tensor perturbations

As can be seen by Eqs. (20) and (36), the scalar and tensor perturbations are stable if the conditions  $z(t)^2 > 0$  and  $z_T(t)^2 > 0$  are satisfied, respectively. Recall that  $z(t)$  and  $z_T(t)$  have the following expressions:

$$z(t)^2 = \frac{a(t)^2}{\left(H(t) + \frac{1}{2f'(R)} \frac{df'(R)}{dt}\right)^2} \left[ \frac{2E\sqrt{G}}{a^3} + \frac{3}{2f'(R)} \left(\frac{df'(R)}{dt}\right)^2 \right], \quad (53)$$

and

$$z_T(t)^2 = a^2 f'(R), \quad (54)$$

as shown in Eqs. (21) and (37). However, as we mentioned earlier, the stability condition has to be checked for all cosmic times, including the bouncing point which occurs

at  $t = 0$ , where the low-curvature approximation no longer holds true. Thus, it will not be justified if we use the form of  $F(R)$  obtained in Eq. (17) to check the stability near the bouncing point. On the other hand, if we find the form of  $F(R)$  in the large-curvature regime ( $R/a_0 \gtrsim 1$ ), then such form of  $F(R)$  cannot be used to examine the stability away from the bouncing point. Thereby, the best way to investigate the stability condition is to determine the forms of  $F(R)$  and  $G(R)$  for the whole range of time  $-\infty < t < \infty$ , and then use such forms of  $F(R)$ ,  $G(R)$  in the expression of  $z(t)$  and  $z_T(t)$ . For this purpose, we solve Eqs. (7) and (8) numerically, and proceed as follows: First we analytically solve Eqs. (7) and (8) in the large-curvature limit ( $\frac{R}{a_0} \gtrsim 1$ ) to estimate the boundary conditions necessary for the numerical solution. Using such boundary conditions, we then solve the equations numerically.

### 1. The large curvature limit

In the large-curvature limit (or equivalently the small cosmic time limit), the scale factor in Eq. (9) becomes

$$a(t) = 1 + a_0 n t^2. \quad (55)$$

The corresponding Hubble rate and the Ricci scalar reads

$$H(t) = 2na_0 t, \quad R(t) = 12na_0[1 + (4n - 3)a_0 t^2]. \quad (56)$$

The above expression for the Ricci scalar can be easily inverted to get the function  $t = t(R)$ , by which we determine the Hubble rate, its first derivative, and the differential operators expressed in terms of  $R$  (with the condition  $\frac{R}{a_0} \gtrsim 1$ ) as follows:

$$H(R) = \sqrt{\frac{n(R - 12na_0)}{3(4n - 3)}},$$

$$\dot{H}(R) = 2na_0 - \frac{(R - 12na_0)}{2(4n - 3)}, \quad (57)$$

$$H \frac{d}{dt} = 4na_0(R - 12na_0) \frac{d}{dR},$$

$$\frac{d^2}{dt^2} = 24na_0^2(4n - 3) \frac{d}{dR}$$

$$+ 48na_0^2(4n - 3)(R - 12na_0) \frac{d^2}{dR^2}. \quad (58)$$

With the above expressions, the gravitational equations (7) and (8) become

$$12na_0(12na_0 - R)J''(R)$$

$$+ 3 \left[ 2na_0 - \frac{(12na_0 - R)}{(3 - 4n)} \left( \frac{1}{2} - \frac{n}{3} \right) \right] J'(R) - \frac{J(R)}{2} = 0, \quad (59)$$

and

$$F(R)/2 = \left[ 2na_0 + \left( n - \frac{1}{2} \right) \frac{(12na_0 - R)}{(3 - 4n)} \right] J'(R)$$

$$+ [8na_0(12na_0 - R) + 24na_0^2(3 - 4n)] J''(R)$$

$$- 48na_0^2(3 - 4n)(12na_0 - R) J'''(R), \quad (60)$$

respectively, with  $J(R) = F(R) + \frac{2E\sqrt{G(R)}}{a^3(R)}$ . The solution of Eq. (59) is given in terms of the confluent hypergeometric function as follows:

$$J(R) = d \left( \frac{2R}{a_0} \right)^{3/2} U \left[ -\frac{(3 + 2n)}{2(3 - 2n)}, \frac{5}{2}, -\frac{(3 - 2n)}{2(3 - 4n)} \right.$$

$$\left. + \frac{(3 - 2n)R/a_0}{24n(3 - 4n)} \right], \quad (61)$$

where  $d$  is an integration constant and has mass dimension  $[+2]$ . The asymptotic behavior of the confluent hypergeometric function is given by  $U[a, b, x] \sim x^{-a}$  when  $x$  is large and thus, in the large curvature limit, the solution  $J(R)$  becomes

$$J(R) \sim d 2^{3/2} \left[ \frac{(3 - 2n)}{24n(3 - 4n)} \right]^{\frac{(3+2n)}{2(3-2n)}} \left( \frac{R}{a_0} \right)^{(6-2n)/(3-2n)}. \quad (62)$$

Since the mass dimension of the integration constant  $d$  is  $[+2]$ , without loss of generality we can take  $d$  as  $d = \frac{a_0}{2^{3/2}} \left[ \frac{24n(3-4n)}{(3-2n)} \right]^{\frac{(3+2n)}{2(3-2n)}}$  (as  $a_0$  also has a mass dimension  $[+2]$ ), which immediately leads to the form of  $J(R)$  as

$$J(R) \sim a_0 \left( \frac{R}{a_0} \right)^{(6-2n)/(3-2n)}. \quad (63)$$

Consequently the form of  $F(R)$  can be obtained from Eq. (60), and is given by the following expression:

$$F(R) \sim a_0 \frac{(1 - 2n)(6 - 2n)}{(3 - 2n)(3 - 4n)} \left( \frac{R}{a_0} \right)^{(6-2n)/(3-2n)}. \quad (64)$$

Thus the effective form of  $f(R)$  is expressed as follows:

$$f(R) = F(R) + \frac{E\sqrt{G(R)}}{a^3(R)} = \frac{1}{2} [J(R) + F(R)]$$

$$\sim a_0 \left[ 1 + \frac{(1 - 2n)(6 - 2n)}{(3 - 2n)(3 - 4n)} \right] \left( \frac{R}{a_0} \right)^{(6-2n)/(3-2n)}. \quad (65)$$

Equations (18) and (65) indicate that in the low-curvature regime,  $f(R)$  goes as  $f(R) \propto R^\rho$ , and in the large-curvature regime  $f(R) \propto R^{(6-2n)/(3-2n)}$ . Recall,  $\rho = \frac{1}{4}[3 - 2n - \sqrt{1 + 4n(5 + n)}]$  which is negative for  $n > 0.25$ , and as

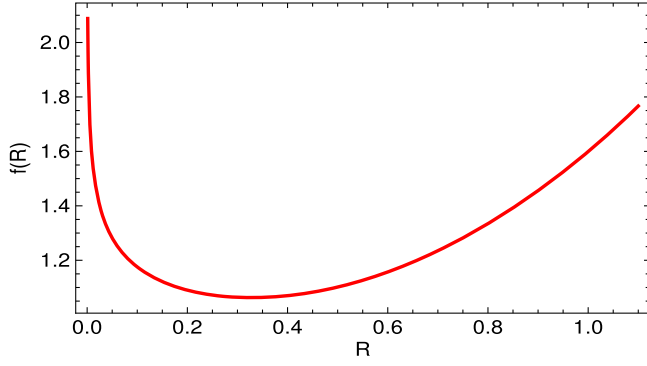


FIG. 4. Numerical solution of  $f = f(R)$  with  $R$  being the independent variable. We take  $a_0 = 1$  (in reduced Planck unit) and  $n = 1/3$ .

shown earlier, the present model is consistent with the Planck results for  $0.27 \lesssim n \lesssim 0.4$ , hence  $\rho$  is negative, in order to ensure the viability of the model. Furthermore,  $\frac{(6-2n)}{3-2n}$  which is the exponent in the large-curvature expression of  $f(R)$  is greater than unity. Therefore, it is clear that in the low-curvature regime  $f(R)$  is proportional to an inverse power of Ricci scalar  $\propto R^{-|\rho|}$ , while in the large-curvature limit,  $f(R)$  is given by a higher power of  $R$ . Such functional forms of  $f(R)$  gravity are used quite frequently in the literature, since they allow unification of early with late-time acceleration. However, in the present paper, we get such form of  $f(R)$  in the context of a symmetric bouncing Universe, where the scale factor evolves as  $a(t) = (a_0 t^2 + 1)^n$ .

## 2. Numerical study of the stability of perturbations

Now we proceed to the numerical solution study of the stability of the perturbations. Using the above forms of  $J(R)$  and  $F(R)$  as boundary conditions along with the expression  $R(t) = 12n \left[ \frac{(4n-1)t^2 + 1/a_0}{(t^2 + 1/a_0)^2} \right]$ , we solve Eqs. (7) and (8) numerically, with the cosmic time  $t$  being the

independent variable. Moreover,  $a_0$  and  $n$  are taken as  $a_0 = 1$  (in reduced Planck units) and  $n = 1/3$ , respectively, so in effect we consider the matter bounce scenario. However, it may be mentioned that the  $n = 1/3$  case makes the model consistent with the Planck 2018 constraints, as confirmed in the previous section. The numerical solution of  $f(R)$  in terms of  $R$  is obtained by using the expression  $R(t) = 12n \left[ \frac{(4n-1)t^2 + 1/a_0}{(t^2 + 1/a_0)^2} \right]$  and is presented in Fig. 4.

It is evident from Fig. 4 that  $f(R)$  decreases in the regime  $R/a_0 \ll 1$ , while in  $R/a_0 \gtrsim 1$ ,  $f(R)$  increases as a function of the Ricci scalar. This is expected from the analytic solutions of  $f(R)$  in the two limiting cases; see Eqs. (18) and (65). In the small and large-curvature regimes,  $f'(R)$  is given by  $\frac{-|\rho|}{R^{1+|\rho|}} < 0$  and  $\frac{(6-2n)}{(3-2n)} R^{3/(3-2n)} > 0$ , respectively, which justify the numerical solution of  $f(R)$  in Fig. 4.

By plugging this numerical solution of  $f(R)$  into the expressions of  $z(t)^2$  and  $z_T(t)^2$ , we can check the stability condition of the metric perturbations for a wide range of the cosmic time. It may be noticed that  $z(t)^2$  and  $z_T(t)^2$  carry a common factor  $a(t)^2$  which is always positive. Thus the stability condition of the scalar and tensor perturbations are given by  $z(t)^2/a(t)^2 > 0$  and  $z_T(t)^2/a(t)^2 > 0$ , respectively. Using the numerical solution shown in Fig. 4, we give plots for  $z(t)^2/a(t)^2$  and  $z_T(t)^2/a(t)^2$  (with respect to the cosmic time) in the left and right plots of Fig. 5, respectively, where we take  $a_0 = 1$  and  $n = 1/3$ . From Fig. 5 it is evident that both the scalar and tensor perturbations are stable in the present context. Moreover, as we mentioned earlier, the squared speed of the perturbations are unity (i.e.,  $c_s^2 = c_T^2 = 1$ ) which guarantees the absence of any ghost modes from the present model. Thus for the matter bounce scenario materialized with the Lagrange multiplier  $F(R)$  gravity model, there exists a range of the free parameters, for which the model becomes compatible with the latest Planck 2018 observations, and also becomes free from instabilities of the metric perturbations.

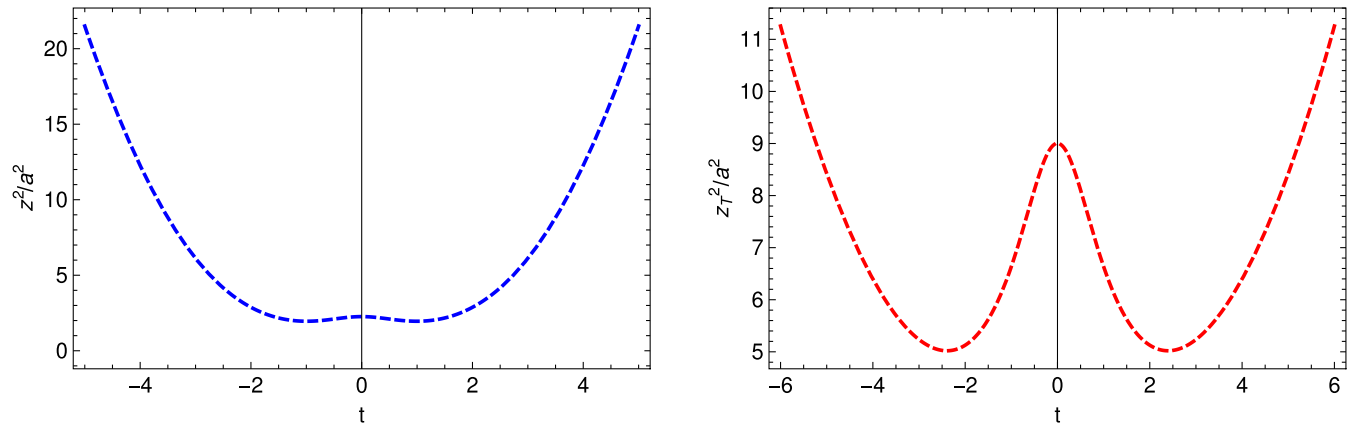


FIG. 5. Left:  $z^2/a^2$  vs  $t$  for the purpose of the stability of the scalar perturbation. Right:  $z_T^2/a^2$  vs  $t$  for the purpose of stability of the tensor perturbation. In both cases, we take  $a_0 = 1$  (in the reduced Planck unit) and  $n = 1/3$ .

## V. ENERGY CONDITION

A crucial drawback in most of the bouncing models is the violation of the null energy condition, which is also a vital ingredient of the Hawking-Penrose theorems, in the context of Einstein's general relativity. Here we check the energy conditions in the context of the Lagrange multiplier  $F(R)$  gravity model. For this purpose, we determine the effective energy density  $\rho_{\text{eff}}$  and pressure  $p_{\text{eff}}$  from Eqs. (7) and (8), as follows:

$$\begin{aligned} \rho_{\text{eff}} &= \frac{1}{2(F'(R) + \frac{EG'}{a^3\sqrt{G}})} \left[ F(R) - \frac{E\sqrt{G}}{a^3} \right. \\ &\quad \left. + 3 \left( \frac{d^2}{dt^2} + H \frac{d}{dt} \right) \left( F'(R) + \frac{EG'}{a^3\sqrt{G}} \right) \right], \\ \rho_{\text{eff}} + p_{\text{eff}} &= -\frac{1}{(F'(R) + \frac{EG'}{a^3\sqrt{G}})} \left[ \frac{E\sqrt{G}}{a^3} + \left( -\frac{d^2}{dt^2} + H \frac{d}{dt} \right) \right. \\ &\quad \left. \times \left( F'(R) + \frac{EG'}{a^3\sqrt{G}} \right) \right]. \end{aligned} \quad (66)$$

By using the above expressions along with the numerical solution of  $f(R)$  determined in the previous section, we give the plots of  $\rho_{\text{eff}}$  and  $\rho_{\text{eff}} + p_{\text{eff}}$  (with respect to cosmic time) in the left and right plots of Fig. 6, respectively, for  $n = 1/3$ ,  $E = 1$ ,  $a_0 = 1$  (in reduced Planck units). As it can be seen in Fig. 6,  $\rho_{\text{eff}}$  remains positive for the whole time regime (or equal to zero at the bouncing point), while  $\rho_{\text{eff}} + p_{\text{eff}}$  becomes negative near the bouncing point. This indicates that the null energy condition is violated, which further implies that the weak energy condition is necessarily violated. At this stage, we want to mention that the holonomy-corrected generalized  $F(R)$  gravity model or the presence of extra spatial dimension, where  $H^2$  is proportional to linear powers, as well as quadratic powers of the

energy density, may play a significant role to rescue the null energy condition for a nonsingular bounce.

However before moving to the next section, we want to state that the present paper studies ‘‘quasimatter bounce’’ in a Lagrange multiplier  $F(R)$  gravity model, which is found to yield a nearly scale-invariant power spectra of scalar and tensor perturbations adiabatically. However, at the background level of the contracting era, it is also known that matter (or quasimatter) contraction is not an attractor, and worse, it is unstable to the growth of anisotropies (more explicitly the anisotropy grows with the scale factor as  $1/a^6$  which is known as the Belinskii-Khalatnikov-Lifshitz (BKL) instability; see [87,88]). Thus the present model remains at the level of a toy model with this respect. However in the ekpyrotic bounce scenario (instead of matter or quasimatter bounce) [17,89,90], the BKL instability does not occur and it will be an interesting avenue to explore the possible effects of a Lagrange multiplier term in an ekpyrotic bounce scenario, which is expected to be studied in a near future work.

## VI. STANDARD $F(R)$ GRAVITY AND THE COMPARISON WITH LAGRANGE MULTIPLIER $F(R)$ GRAVITY

In this section, we consider the standard  $F(R)$  gravity to study the realization of the bouncing universe of Eq. (9) and we shall compare the results with those obtained for the Lagrange multiplier  $F(R)$  gravity model. The action for a vacuum  $F(R)$  gravity model is given by

$$S = \frac{1}{2\kappa^2} \int d^4x \sqrt{-g} F(R), \quad (67)$$

where  $\frac{1}{\kappa^2} = M^2$  with  $M$  being again the four-dimensional Planck mass. The action in Eq. (67) leads to the following Friedmann equations of motion:

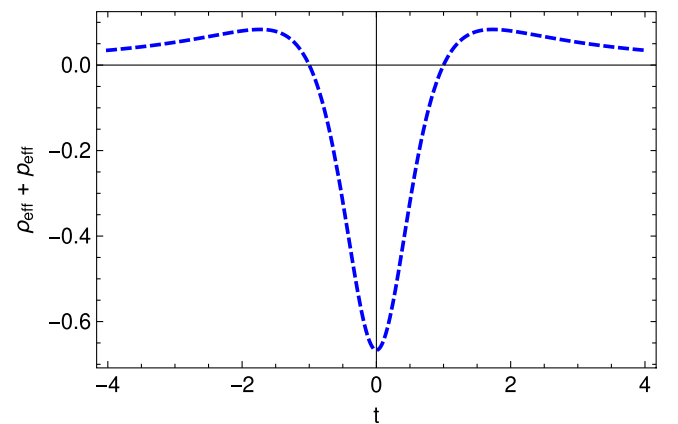
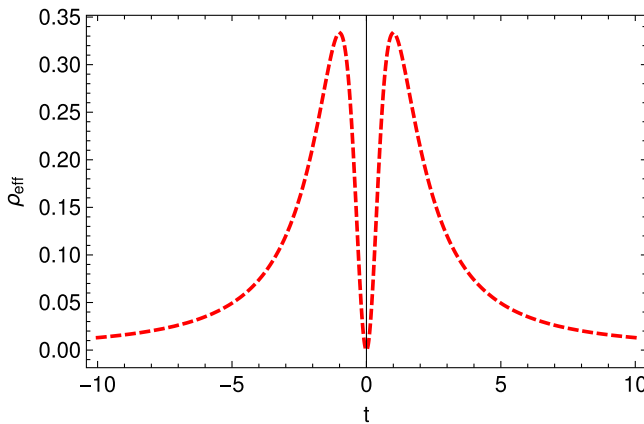


FIG. 6. Left:  $\rho_{\text{eff}}$  vs  $t$  for the purpose of weak energy condition. Right:  $\rho_{\text{eff}} + p_{\text{eff}}$  vs  $t$  for the purpose of null energy condition. In both cases, we take  $E = 1$ ,  $a_0 = 1$  (in reduced Planck units) and  $n = 1/3$ .

$$\begin{aligned} -\frac{F(R)}{2} + 3(\dot{H} + H^2)F'(R) - 3H\frac{dF'}{dt} &= 0, \\ \frac{F(R)}{2} - (\dot{H} + 3H^2)F'(R) + \left(\frac{d^2}{dt^2} + 2H\frac{d}{dt}\right)F'(R) &= 0, \end{aligned} \quad (68)$$

with  $H$  being the Hubble rate. We should note that Eqs. (7) and (8) become identical with Eq. (68) by choosing  $E = 0$ , since for  $E = 0$ , the Lagrange multiplier field  $\lambda(t)$  goes to zero and thus the gravitational equations of a Lagrange multiplier  $F(R)$  gravity model become identical with that of a standard  $F(R)$  gravity. As we discussed earlier, for the purpose of determining the observable quantities, the low-curvature limit i.e.,  $R/a_0 \ll 1$ , is a viable approximation. Recall that, in the regime  $R/a_0 \ll 1$ , the Ricci scalar can be written as  $R(t) = \frac{12n(4n-1)}{t^2}$ . This along with the expressions of the Hubble rate, its first derivative, and the differential operators, as determined in Eq. (13), will enable us to express the gravitational equations as follows:

$$\frac{2}{(4n-1)}R^2F''(R) - \frac{(1-2n)}{(4n-1)}RF'(R) - F(R) = 0, \quad (69)$$

which can be solved as

$$F(R) = a_0 \left[ \left(\frac{R}{a_0}\right)^\rho + \left(\frac{R}{a_0}\right)^\delta \right], \quad (70)$$

with  $\rho = \frac{1}{4}[3 - 2n - \sqrt{1 + 4n(5+n)}]$  and  $\delta = \frac{1}{4}[3 - 2n + \sqrt{1 + 4n(5+n)}]$ . Equation (70) represents the reconstructed form of  $F(R)$  gravity for the bouncing scale factor  $a(t) = (a_0 t^2 + 1)^n$ . This form of  $F(R)$  matches with the reconstructed form of effective  $f(R)$  [see Eq. (18), apart from the coefficients] in a Lagrange multiplier higher curvature model in the low curvature regime.

Before moving towards the perturbation, at this stage we want to study whether this form of  $F(R)$  [in Eq. (70)] passes the astrophysical tests in low curvature regime. An example of the test is matter instability, which is related to the fact that the spherical body solution in general relativity may not be the solution in modified gravity theory. The matter instability may appear when the energy density or the curvature is large compared with the average density or curvature in the universe, as is the case inside of a planet. Following [77], we immediately write the potential [ $U(R_b)$ , with  $R_b$  being the perturbed Ricci scalar] for the perturbed Ricci curvature over Einstein gravity as

$$\begin{aligned} U(R_b) &= \frac{R_b}{3} - \frac{F^{(1)}(R_b)F^{(3)}(R_b)R_b}{3F^{(2)}(R_b)^2} - \frac{F^{(1)}(R_b)}{3F^{(2)}(R_b)} \\ &+ \frac{2F(R_b)F^{(3)}(R_b)}{3F^{(2)}(R_b)^2} - \frac{F^{(3)}(R_b)R_b}{3F^{(2)}(R_b)^2} \end{aligned} \quad (71)$$

where we denote  $d^k F(R)/dR^k = F^{(k)}(R)$ . If  $U(R_b) > 0$ , the perturbation grows with time, and the system becomes unstable. Recall  $\rho < 0$  and  $\delta > 0$  and thus the term  $R^\rho$  dominates over  $R^\delta$  in the low curvature regime. Thus we can approximate  $F(R) \sim R^\rho$  in the low curvature regime which immediately leads to the potential as

$$U(R_b) = -\frac{2(|\rho| + 2)}{9|\rho|(|\rho| + 1)}R_b + \frac{(|\rho| + 2)}{3|\rho|(|\rho| + 1)}R_b^{2+|\rho|}. \quad (72)$$

In the low curvature regime, the first term dominates in the above expression of  $U(R_b)$  and thus  $U(R_b)$  becomes less than zero. This indicates that the model considered here passes the matter instability test. However more checks of this theory should be done in order to conclude if the model is a realistic one or not, which we expect to study in a future work.

Having the reconstructed form of  $F(R)$  in hand, we proceed to study the cosmological perturbations in this model and the perturbed metric is given by

$$ds^2 = -(1 + 2\tilde{\Psi})dt^2 + a(t)^2(1 - 2\tilde{\Psi})(\delta_{ij} + \tilde{h}_{ij})dx^i dx^j, \quad (73)$$

where  $\tilde{\Psi}(t, \vec{x})$  and  $\tilde{h}_{ij}(t, \vec{x})$  are scalar and tensor perturbed variable, respectively. The tilde quantities are reserved for the pure  $F(R)$  gravity model, in order to make a comparison with the Lagrange multiplier  $F(R)$  gravity model. Using the same procedure as discussed in Sec. IV, we obtain the first order perturbed equations in the  $F(R)$  gravity model as follows:

$$\begin{aligned} \frac{d^2 \tilde{v}}{d\tau^2} + \left[ k^2 - \frac{1}{\tilde{z}} \frac{d^2 \tilde{z}}{d\tau^2} \right] \tilde{v}(\tau) &= 0, \\ \frac{d^2 \tilde{v}_T}{d\tau^2} + \left[ k^2 - \frac{1}{\tilde{z}_T} \frac{d^2 \tilde{z}_T}{d\tau^2} \right] \tilde{v}_T(\tau) &= 0, \end{aligned} \quad (74)$$

where  $\tau$  is the conformal time given by  $\tau = \frac{t^{1-2n}}{a_0^{1-2n}}$ . Moreover  $\tilde{z}(\tau)$ ,  $\tilde{z}_T(\tau)$  are the scalar, tensor type Mukhanov-Sasaki variable, respectively, and have the following forms:

$$\begin{aligned} \tilde{z}[\tau(t)] &= \frac{a(t)}{(H(t) + \frac{1}{2F'(R)} \frac{dF'(R)}{dt})} \sqrt{\frac{3}{2F'(R)} \left( \frac{dF'(R)}{dt} \right)^2}, \\ \tilde{z}_T[\tau(t)] &= a\sqrt{F'(R)}. \end{aligned} \quad (75)$$

Comparing the above expression with Eqs. (21) and (37), it is clearly observed that for  $E = 0$ , the scalar and tensor type Mukhanov-Sasaki variables in a standard  $F(R)$  gravity model become the same as that of the Lagrange multiplier  $F(R)$  gravity model, as expected. Using Eq. (75), we further obtain the following expressions (in the low-curvature regime) which are important towards solving the Mukhanov equations:

$$\frac{1}{\tilde{z}} \frac{d^2 \tilde{z}}{d\tau^2} = \frac{\xi(\xi-1)}{\tau^2} \left[ 1 + \frac{2(\delta-\rho)}{(\xi-1)} (R/a_0)^{\delta-\rho} \left( \frac{\delta(\rho-\delta)}{\rho(2n-\rho+1)} + \frac{\delta(1+\rho-2\delta)}{\rho(1-\rho)} \right) \right], \quad (76)$$

and

$$\frac{1}{\tilde{z}_T} \frac{d^2 \tilde{z}_T}{d\tau^2} = \frac{\xi(\xi-1)}{\tau^2} \left[ 1 - \frac{2\delta(\delta-\rho)}{(\xi-1)\rho} (R/a_0)^{\delta-\rho} \right], \quad (77)$$

and recall that  $\xi = \frac{(2n+1-\rho)}{(1-2n)}$ . As  $\delta - \rho$  is a positive quantity, the terms in the parentheses in Eqs. (76) and (77), can be safely considered to be small in the low-curvature regime and consequently  $\tilde{z}''(\tau)/\tilde{z}$  and  $\tilde{z}_T''(\tau)/\tilde{z}_T$  become proportional to  $1/\tau^2$ . In effect, the solutions of the Mukhanov variables are expressed in terms of the Hankel function as discussed earlier in Sec. IV. With these solutions, we obtain the spectral index  $\tilde{n}_s$  and the tensor-to-scalar ratio  $\tilde{r}$  for the standard  $F(R)$  gravity model as follows:

$$\tilde{n}_s = 4 - \sqrt{1 + 4\xi(\xi-1) \left[ 1 + \frac{2(\delta-\rho)}{(\xi-1)} (R_h/a_0)^{\delta-\rho} \left( \frac{\delta(\rho-\delta)}{\rho(2n-\rho+1)} + \frac{\delta(1+\rho-2\delta)}{\rho(1-\rho)} \right) \right]}, \quad (78)$$

and

$$\tilde{r} = 2 \left[ \frac{\tilde{z}(\tau)}{\tilde{z}_T(\tau)} \right]^2 \Big|_{\tau=\tau_h} = 3 \left[ \frac{1}{F'(R)(H(t) + \frac{1}{2F'(R)} \frac{dF'(R)}{dt})} \right]^2 \left( \frac{dF'(R)}{dt} \right)^2 \Big|_{t=t_h}, \quad (79)$$

respectively, where  $t_h$  is the time of horizon exit and  $R_h = R(t_h)$ . Similarly to the previously discussed Lagrange multiplier  $F(R)$  gravity model, see Sec. IV, the spectral index and tensor to scalar ratio of the  $F(R)$  gravity model depend on the parameters  $R_h/a_0$  and  $n$  (both are dimensionless parameters). With these expressions, we can confront the observational parameters of the models with the Planck 2018 results. For the  $F(R)$  gravity model, the spectral index ( $\tilde{n}_s$ ) lies within the Planck constraints for a narrow regime of the parameters as  $10^{-4} \lesssim \frac{R_h}{a_0} \lesssim 3 \times 10^{-4}$  and  $0.1860 \leq n \leq 0.1866$ . However for these values of the free parameters, the tensor-to-scalar ratio takes values in the range  $1.9915 \lesssim \tilde{r} \lesssim 1.9940$  and hence is not compatible with the Planck results. Thereby, we can argue that  $\tilde{n}_s$  and  $\tilde{r}$  are not simultaneously compatible with the Planck constraints for a bouncing universe [with  $a(t) = (a_0 t^2 + 1)^n$ ] in the standard  $F(R)$  model, in contrast to the Lagrange multiplier  $F(R)$  gravity model. This clearly indicates the importance of the Lagrange multiplier field  $\lambda(t)$ , present in action (1) in making the compatibility of the observational parameters with the Planck results. Furthermore the running of the spectral index is determined as

$$\begin{aligned} \tilde{\alpha} &= \frac{dn_s}{d \ln k} \Big|_{\tau=\tau_h} \\ &= \frac{4\xi(\delta-\rho)^2}{\sqrt{1+4\xi(\xi-1)}} \left( \frac{R_h}{a_0} \right)^{\delta-\rho} \left( \frac{\delta(\rho-\delta)}{\rho(2n-\rho+1)} + \frac{\delta(1+\rho-2\delta)}{\rho(1-\rho)} \right), \end{aligned} \quad (80)$$

where we used the relation of horizon crossing of the  $k$ th mode, that is  $k = aH$ . It turns out that  $\tilde{\alpha}$  lies within the Planck constraints  $\alpha = -0.0085 \pm 0.0073$  for  $0.1860 \leq n \leq 0.1866$  along with  $R_h/a_0 = 2 \times 10^{-4}$  (the regime where  $\tilde{n}_s$  is also compatible with the Planck results) and this is demonstrated in Fig. 7. Thus in conclusion, in the  $F(R)$  model, the spectral index and the running index are consistent with the Planck results while the tensor-to-scalar ratio is not. However, the presence of the field  $\lambda(t)$  in the  $F(R)$  gravity model makes all three parameters simultaneously compatible with observational constraints. This makes it clear that the field  $\lambda(t)$  has a significant contribution on the observational parameters. Next we proceed to explore the stability condition of the  $F(R)$  model. In order to investigate the stability condition, we need to determine the form of  $F(R)$  for the whole duration of the bounce, and for this purpose we solve Eq. (68) numerically. However, before going to the numerical solution,

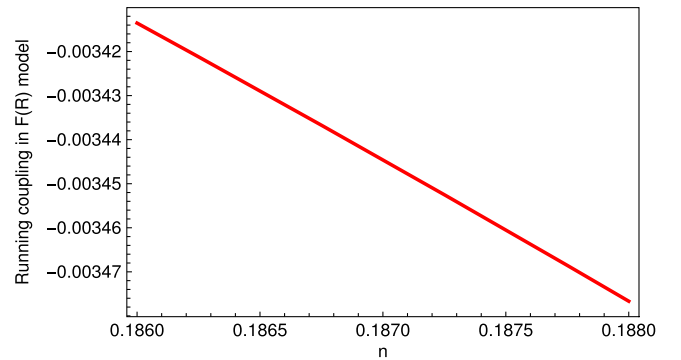


FIG. 7. Parametric plot of  $\tilde{\alpha}$  vs  $n$  for  $R_h/a_0 = 2 \times 10^{-4}$ .

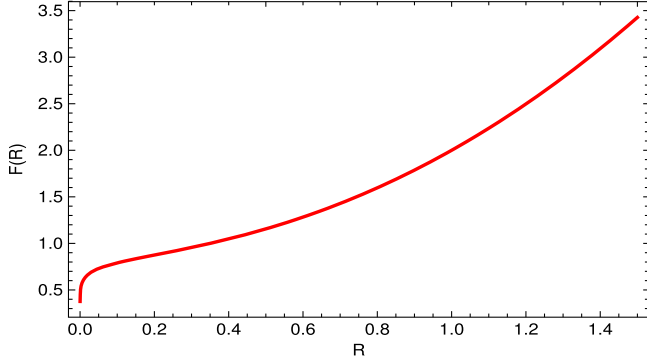


FIG. 8. Numerical solution of  $F(R)$  with  $n = 0.186$  and  $a_0 = 1$ .

we reconstruct the form of  $F(R)$  for  $a(t) = (a_0 t^2 + 1)^n$  in the large-curvature regime  $R/a_0 \gtrsim 1$ , which will act as boundary condition in determining the numerical solution. In the large curvature regime the  $F(R)$  gravitational equation becomes

$$12na_0(12na_0 - R)F''(R) + 3 \left[ 2na_0 - \frac{(12na_0 - R)}{(3 - 4n)} \left( \frac{1}{2} - \frac{n}{3} \right) \right] F'(R) - \frac{F(R)}{2} = 0. \quad (81)$$

The solution of Eq. (81) is given in terms of the hypergeometric function, and by using the asymptotic behavior of the hypergeometric function, we can write the solution of  $F(R)$  in regime  $R/a_0 \gtrsim 1$  as follows:

$$F(R) \sim a_0 \left( \frac{R}{a_0} \right)^{(6-2n)/(3-2n)}. \quad (82)$$

By using the above expression as a boundary condition along with  $a_0 = 1$ ,  $n = 0.186$ , we obtain the numerical solution of  $F(R)$  from Eq. (68). This is depicted in Fig. 8. As it can be seen in Fig. 8, the  $F(R)$  starts from zero (at  $R \sim 0$ ) and gradually increases with the Ricci scalar, unlike the case of the Lagrange multiplier  $F(R)$  gravity model,

where  $f(R)$  actually diverges at  $R = 0$  (see Fig. 4). This feature occurs due to the different viability regime of the parameter  $n$ , which makes the corresponding model consistent with the Planck results. In the Lagrange multiplier  $F(R)$  gravity model, the viability range of  $n$  is given by  $0.27 \lesssim n \lesssim 0.40$ , which makes  $\rho (= \frac{1}{4}[3 - 2n - \sqrt{1 + 4n(5 + n)}])$  a negative quantity. Thus the effective  $f(R)$  behaves as an inverse power of  $R$  in the low-curvature regime and diverges at  $R = 0$ , as shown in Fig. 4. On the other hand, for the standard  $F(R)$  model the viability regime of  $n$ , in terms of spectral index and running index, is given by  $0.1860 \lesssim n \lesssim 0.1866$  which makes  $\rho$  a positive quantity. As a result  $F(R)$  behaves as a positive power of  $R$  in the low-curvature regime and goes to zero at  $R = 0$ , as depicted in Fig. 8. By using the numerical solution of  $F(R)$ , we give the plots of  $\tilde{z}^2/a^2$  and  $\tilde{z}_T^2/a^2$  (with respect to time) in the left and right plots of Fig. 9 to check the stability of the scalar ( $\tilde{\Psi}$ ) and tensor ( $\tilde{h}_{ij}$ ) perturbation, respectively. Figure 9 clearly reveals that, for the  $F(R)$  model at hand, the scalar perturbation is not stable while the tensor perturbation is, in contrast to the case of the generalized Lagrange multiplier  $F(R)$  gravity, where both the scalar and tensor perturbations are found to be stable; see Fig. 5. Actually, the absence of the Lagrange multiplier field destabilizes the scalar perturbations without affecting though the stability of the tensor perturbations. Regarding the energy conditions in the  $F(R)$  model, it turns out that the weak energy condition is satisfied while the null energy condition is violated near the bouncing point, for the bouncing universe described by  $a(t) = (a_0 t^2 + 1)^n$ . The comparison of the standard vacuum  $F(R)$  gravity with that of the Lagrange multiplier  $F(R)$  gravity is shown in Table I.

Thus the bouncing universe with  $a(t) = (a_0 t^2 + 1)^n$  is well described by the Lagrange multiplier  $F(R)$  model in comparison to the standard  $F(R)$  gravity. However the presence of the Lagrange multiplier field cannot rescue the null energy condition. In this regard, we want to mention that the holonomy corrected generalized  $F(R)$  gravity

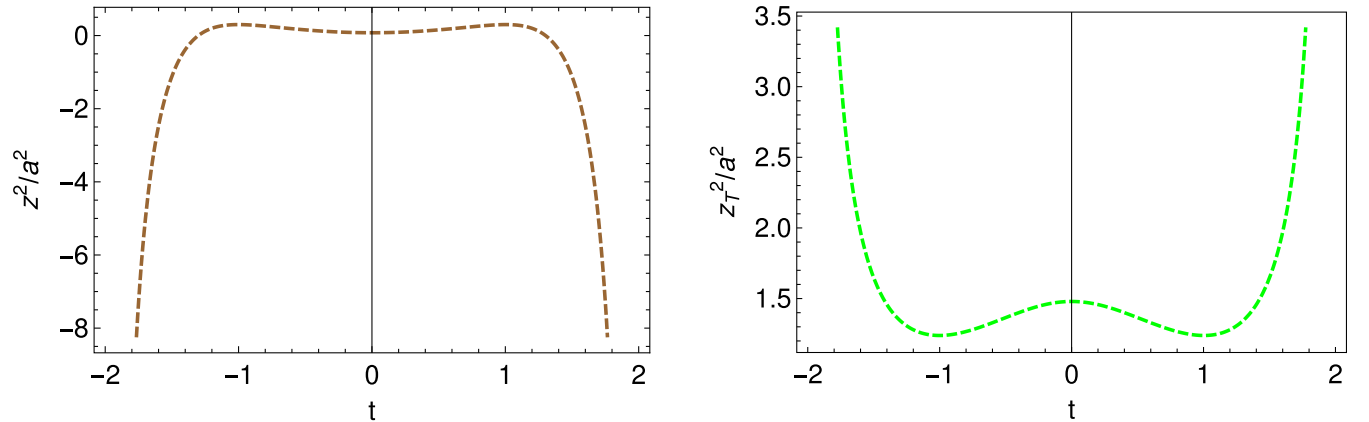


FIG. 9. Left:  $z^2/a^2$  vs  $t$  for the purpose of the stability of the scalar perturbation. Right:  $z_T^2/a^2$  vs  $t$  for the purpose of stability of the tensor perturbation. In both cases, we take  $a_0 = 1$  (in reduced Planck units) and  $n = 0.186$ .

TABLE I. Comparison of observable quantities, stability of the perturbations, and the energy conditions for the Lagrange multiplier  $F(R)$  model and the standard  $F(R)$  gravity.

Observable quantities, stability of energy conditions	Lagrange multiplier $F(R)$ model	Standard $F(R)$ model
1. Observable quantities	Viable	Not viable
2. Scalar perturbation	Stable	Not stable
3. Tensor perturbation	Stable	Stable
4. Weak energy condition	Violated	Violated
5. Null energy condition	Violated	Violated

where  $H^2$  is proportional to linear as well as squared of the effective energy density, may rescue the energy condition and we defer this task to a near future work.

## VII. COMOVING HUBBLE RADIUS: VIABILITY OF THE LOW-CURVATURE LIMIT

Before concluding, let us comment on an interesting issue, related to the viability of the low-curvature approximation that we have considered in calculating the scalar and tensor power spectrum in Sec. IV. In the context of the matter bounce cosmology, which is obtained by taking  $n = 1/3$  in Eq. (9), the primordial perturbations of the comoving curvature, which originate from quantum vacuum fluctuations, were at subhorizon scales during the contracting era in the low-curvature regime, that is, their wavelength was much smaller than the comoving Hubble radius which is defined by  $r_h = \frac{1}{aH}$ . In the matter bounce evolution, the Hubble horizon radius decreases in size, and this causes the perturbation modes to exit from the horizon eventually, with this exit occurring when the contracting Hubble horizon becomes equal to the wavelength of these primordial modes. However, in the present context, we consider a larger class of bouncing models of the form  $a(t) = (a_0 t^2 + 1)^n$ , in the presence of a generalized Lagrange multiplier  $F(R)$  gravity. In such a higher curvature model, it turns out that the observable quantities lie within the Planck constraints when the parameter values are taken in the range  $0.01 \lesssim \frac{R_h}{a_0} \lesssim 0.07$  and  $0.27 \lesssim n \lesssim 0.40$  and moreover, by calculating the observable quantities, we have assumed that the horizon exit of the perturbation modes occurred during the low-curvature regime of the contracting era. Thus, it will be important to check what are the possible values of  $n$  which make the low-curvature limit a viable approximation in calculating the power spectrum for the bouncing model  $a(t) = (a_0 t^2 + 1)^n$ .

The expression of the scale factor in Eq. (9) immediately leads to the comoving Hubble radius,

$$r_h = \frac{(1 + a_0 t^2)^{1-n}}{2a_0 n t}. \quad (83)$$

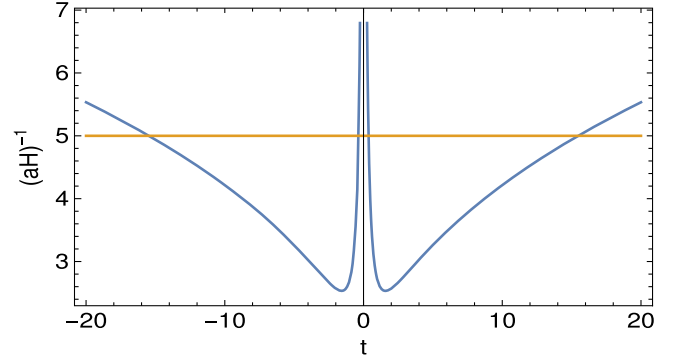


FIG. 10. Comoving Hubble radius (blue curve) and a perturbation mode (yellow curve) with respect to cosmic time for  $n = 0.30$ .

Thereby  $r_h$  diverges at  $t \simeq 0$ , as expected because the Hubble rate goes to zero at the bouncing point. Furthermore, the asymptotic behavior of  $r_h$  is given by  $r_h \sim t^{1-2n}$ , thus  $r_h(|t| \rightarrow \infty)$  diverges for  $n < 1/2$ , otherwise  $r_h$  goes to zero asymptotically. Hence, for  $n < 1/2$ , the comoving Hubble radius decreases initially in the contracting era and then diverges near the bouncing point, unlike in the case  $n > 1/2$  where the Hubble radius increases from the infinite past and gradually diverges at  $t = 0$ . As a result, the possible range of  $n$  which leads the perturbation modes to exit the horizon at large negative time and make the low-curvature limit a viable approximation in calculating the power spectrum, is given by  $0 < n < 1/2$ . Moreover this range of  $n$  also supports the range  $0.27 \lesssim n \lesssim 0.40$ , which makes the observable quantities simultaneously compatible with the Planck 2018 results. In Fig. 10 we plot the comoving Hubble radius and a perturbation mode as functions of the cosmic time for  $n = 0.30$ .

## VIII. CONCLUSIONS

In this paper, we considered a variant matter bounce cosmology with  $a(t) = (a_0 t^2 + 1)^n$ , in the context of the Lagrange multiplier  $F(R)$  gravity model. For such model, it was shown that for  $n < 1/2$ , the perturbation modes, which were generated during the contracting era, exit from the comoving Hubble radius at large negative time, deeply in the contracting era, which in turn makes the low-curvature limit a viable approximation in calculating the observable quantities. Thus we constructed the form of effective  $f(R)$  gravity that may materialize the above cosmic scenario, and consequently we determined the scalar and tensor power spectrums in the low-curvature regime. These lead to the expressions of various observable quantities like spectral index of primordial scalar perturbations, the tensor-to-scalar ratio, and the running of spectral index, which were found to depend on the dimensionless parameters  $R_h/a_0$  and  $n$ , with  $R_h$  being the Ricci curvature at horizon exit. It turned out that such observable quantities are simultaneously compatible with the Planck 2018 constraints for the parameters chosen

in the range  $0.01 \lesssim \frac{R_h}{a_0} \lesssim 0.07$  and  $0.27 \lesssim n \lesssim 0.40$ . It may be noticed that this range of  $n$  is supported by the range  $0 < n < 1/2$  which makes the low-curvature approximation a valid approximation in calculating the power spectrums. The stability condition of the metric perturbations had to be checked for all cosmic times, including the bouncing point time instance  $t = 0$ , where the low-curvature approximation does not hold true. For the purpose of examining the stability conditions, we determined the  $f(R)$  gravity beyond the low-curvature regime, in particular, for the whole range of time ( $-\infty < t < \infty$ ) by solving the Friedmann equations without the low-curvature approximation, however, numerically. The numerical solution clearly depicted that in the low-curvature regime,  $f(R)$  is proportional to an inverse power of the Ricci scalar, while in the large curvature limit,  $f(R)$  is given by a higher power (higher than one) of  $R$ . Such characteristics of  $f(R)$  gravity have been widely used in the literature mainly in order to unify the early-time with the late-time acceleration.

By using the obtained numerical solutions, we checked the stability conditions and as a result we found that both the scalar and tensor perturbations were stable for the same range of parameter values, which guaranteed the phenomenological viability of the model. Moreover the Mukhanov-Sasaki equations suggest that the squared speed of the gravity waves is unity, which confirmed the absence of any ghost modes. We further calculated the effective energy density and pressure in the present context in order to investigate the energy conditions. As a consequence, we found that both the null energy and the weak energy conditions are violated near the bouncing point. The phenomenology of the present nonsingular bounce is also

discussed in the context of a standard  $F(R)$  gravity model. We found that the results obtained in the Lagrange multiplier  $F(R)$  gravity model are in contrast with the standard  $F(R)$  model for which the spectral index and the running index are simultaneously compatible with the Planck results; however, the tensor-to-scalar ratio is not. Also the scalar perturbation is stable but the model is plagued with the instability of the tensor perturbation and finally, the weak energy condition is satisfied while the null energy condition is violated.

The above features clearly justify the importance of the Lagrange multiplier field in making the observational indices compatible with the Planck data and also in removing the instability of the metric perturbations. Therefore the bouncing universe with  $a(t) = (a_0 t^2 + 1)^n$  is well described by the Lagrange multiplier  $F(R)$  gravity model in comparison to the standard  $F(R)$  model. However the presence of the Lagrange multiplier field cannot evade the violation of null energy condition. In this regard, we want to mention that the holonomy-corrected higher curvature model may rescue the null energy condition and we hope to address this issue in a future work.

## ACKNOWLEDGMENTS

This work is supported by MINECO (Spain), FIS2016-76363-P, and by Project No. 2017 SGR247 (AGAUR, Catalonia) (S. D. O). This work is also supported by MEXT KAKENHI Grant-in-Aid for Scientific Research on Innovative Areas ‘‘Cosmic Acceleration’’ No. 15H05890 (S. N.) and the JSPS Grant-in-Aid for Scientific Research (C) No. 18K03615 (S. N.).

- 
- [1] R. H. Brandenberger, [arXiv:1206.4196](#).
  - [2] R. Brandenberger and P. Peter, [Found. Phys.](#) **47**, 797 (2017).
  - [3] D. Battefeld and P. Peter, [Phys. Rep.](#) **571**, 1 (2015).
  - [4] M. Novello and S. E. P. Bergliaffa, [Phys. Rep.](#) **463**, 127 (2008).
  - [5] Y. F. Cai, [Sci. China Phys. Mech. Astron.](#) **57**, 1414 (2014).
  - [6] J. de Haro and Y. F. Cai, [Gen. Relativ. Gravit.](#) **47**, 95 (2015).
  - [7] J. L. Lehners, [Classical Quantum Gravity](#) **28**, 204004 (2011).
  - [8] J. L. Lehners, [Phys. Rep.](#) **465**, 223 (2008).
  - [9] Y. K. E. Cheung, C. Li, and J. D. Vergados, [Symmetry](#) **8**, 136 (2016).
  - [10] Y. F. Cai, A. Marciano, D. G. Wang, and E. Wilson-Ewing, [Universe](#) **3**, 1 (2016).
  - [11] C. Cattoen and M. Visser, [Classical Quantum Gravity](#) **22**, 4913 (2005).
  - [12] V. F. Mukhanov and R. H. Brandenberger, [Phys. Rev. Lett.](#) **68**, 1969 (1992).
  - [13] C. Li, R. H. Brandenberger, and Y. K. E. Cheung, [Phys. Rev. D](#) **90**, 123535 (2014).
  - [14] D. Brizuela, G. A. D. Mena Marugan, and T. Pawłowski, [Classical Quantum Gravity](#) **27**, 052001 (2010).
  - [15] Y. F. Cai, E. McDonough, F. Duplessis, and R. H. Brandenberger, [J. Cosmol. Astropart. Phys.](#) **10** (2013) 024.
  - [16] J. Quintin, Y. F. Cai, and R. H. Brandenberger, [Phys. Rev. D](#) **90**, 063507 (2014).
  - [17] Y. F. Cai, R. Brandenberger, and P. Peter, [Classical Quantum Gravity](#) **30**, 075019 (2013).
  - [18] N. J. Poplawski, [Phys. Rev. D](#) **85**, 107502 (2012).
  - [19] M. Koehn, J. L. Lehners, and B. Ovrut, [Phys. Rev. D](#) **93**, 103501 (2016).
  - [20] S. D. Odintsov and V. K. Oikonomou, [Phys. Rev. D](#) **92**, 024016 (2015).
  - [21] S. Nojiri, S. D. Odintsov, and V. K. Oikonomou, [Phys. Rev. D](#) **93**, 084050 (2016).
  - [22] V. K. Oikonomou, [Phys. Rev. D](#) **92**, 124027 (2015).

- [23] S. D. Odintsov and V. K. Oikonomou, *Int. J. Mod. Phys. D* **26**, 1750085 (2017).
- [24] M. Koehn, J. L. Lehnert, and B. A. Ovrut, *Phys. Rev. D* **90**, 025005 (2014).
- [25] L. Battarra and J. L. Lehnert, *J. Cosmol. Astropart. Phys.* **12** (2014) 023.
- [26] J. Martin, P. Peter, N. Pinto Neto, and D. J. Schwarz, *Phys. Rev. D* **65**, 123513 (2002).
- [27] J. Khoury, B. A. Ovrut, P. J. Steinhardt, and N. Turok, *Phys. Rev. D* **64**, 123522 (2001).
- [28] E. I. Buchbinder, J. Khoury, and B. A. Ovrut, *Phys. Rev. D* **76**, 123503 (2007).
- [29] M. G. Brown, K. Freese, and W. H. Kinney, *J. Cosmol. Astropart. Phys.* **03** (2008) 002.
- [30] J. C. Hackworth and E. J. Weinberg, *Phys. Rev. D* **71**, 044014 (2005).
- [31] S. Nojiri and S. D. Odintsov, *Phys. Lett. B* **637**, 139 (2006).
- [32] M. C. Johnson and J. L. Lehnert, *Phys. Rev. D* **85**, 103509 (2012).
- [33] P. Peter and N. Pinto-Neto, *Phys. Rev. D* **66**, 063509 (2002).
- [34] M. Gasperini, M. Giovannini, and G. Veneziano, *Phys. Lett. B* **569**, 113 (2003).
- [35] P. Creminelli, A. Nicolis, and M. Zaldarriaga, *Phys. Rev. D* **71**, 063505 (2005).
- [36] J. L. Lehnert and E. Wilson-Ewing, *J. Cosmol. Astropart. Phys.* **10** (2015) 038.
- [37] J. Mielczarek, M. Kamionka, A. Kurek, and M. Szydlowski, *J. Cosmol. Astropart. Phys.* **07** (2010) 004.
- [38] J. L. Lehnert and P. J. Steinhardt, *Phys. Rev. D* **87**, 123533 (2013).
- [39] Y. F. Cai, J. Quintin, E. N. Saridakis, and E. Wilson-Ewing, *J. Cosmol. Astropart. Phys.* **07** (2014) 033.
- [40] Y. F. Cai, T. Qiu, Y. S. Piao, M. Li, and X. Zhang, *J. High Energy Phys.* **10** (2007) 071.
- [41] Y. F. Cai and E. N. Saridakis, *Classical Quantum Gravity* **28**, 035010 (2011).
- [42] P. P. Avelino and R. Z. Ferreira, *Phys. Rev. D* **86**, 041501 (2012).
- [43] J. D. Barrow, D. Kimberly, and J. Magueijo, *Classical Quantum Gravity* **21**, 4289 (2004).
- [44] J. Haro and E. Elizalde, *J. Cosmol. Astropart. Phys.* **10** (2015) 028.
- [45] E. Elizalde, J. Haro, and S. D. Odintsov, *Phys. Rev. D* **91**, 063522 (2015).
- [46] A. Das, D. Maity, T. Paul, and S. SenGupta, *Eur. Phys. J. C* **77**, 813 (2017).
- [47] P. Laguna, *Phys. Rev. D* **75**, 024033 (2007).
- [48] A. Corichi and P. Singh, *Phys. Rev. Lett.* **100**, 161302 (2008).
- [49] M. Bojowald, *Gen. Relativ. Gravit.* **40**, 2659 (2008).
- [50] P. Singh, K. Vandersloot, and G. V. Vereshchagin, *Phys. Rev. D* **74**, 043510 (2006).
- [51] G. Date and G. M. Hossain, *Phys. Rev. Lett.* **94**, 011302 (2005).
- [52] J. de Haro, *J. Cosmol. Astropart. Phys.* **11** (2012) 037.
- [53] F. Cianfrani and G. Montani, *Phys. Rev. D* **82**, 021501 (2010).
- [54] Y. F. Cai and E. Wilson-Ewing, *J. Cosmol. Astropart. Phys.* **03** (2014) 026.
- [55] J. Mielczarek and M. Szydlowski, *Phys. Rev. D* **77**, 124008 (2008).
- [56] J. Mielczarek, T. Stachowiak, and M. Szydlowski, *Phys. Rev. D* **77**, 123506 (2008).
- [57] P. Diener, B. Gupt, and P. Singh, *Classical Quantum Gravity* **31**, 105015 (2014).
- [58] J. Haro, A. N. Makarenko, A. N. Myagky, S. D. Odintsov, and V. K. Oikonomou, *Phys. Rev. D* **92**, 124026 (2015).
- [59] X. Zhang and Y. Ma, *Phys. Rev. D* **84**, 064040 (2011).
- [60] X. Zhang and Y. Ma, *Phys. Rev. Lett.* **106**, 171301 (2011).
- [61] Y. F. Cai and E. Wilson-Ewing, *J. Cosmol. Astropart. Phys.* **03** (2015) 006.
- [62] E. Wilson-Ewing, *J. Cosmol. Astropart. Phys.* **03** (2013) 026.
- [63] F. Finelli and R. Brandenberger, *Phys. Rev. D* **65**, 103522 (2002).
- [64] Y. F. Cai, R. Brandenberger, and X. Zhang, *Phys. Lett. B* **703**, 25 (2011).
- [65] J. Haro and J. Amorós, *Proc. Sci.*, FFP14 (2016) 163 [arXiv:1501.06270].
- [66] Y. F. Cai, R. Brandenberger, and X. Zhang, *J. Cosmol. Astropart. Phys.* **03** (2011) 003.
- [67] J. Haro and J. Amorós, *J. Cosmol. Astropart. Phys.* **12** (2014) 031.
- [68] R. Brandenberger, *Phys. Rev. D* **80**, 043516 (2009).
- [69] J. de Haro and J. Amorós, *J. Cosmol. Astropart. Phys.* **08** (2014) 025.
- [70] S. D. Odintsov and V. K. Oikonomou, *Phys. Rev. D* **90**, 124083 (2014).
- [71] T. Qiu and K. C. Yang, *J. Cosmol. Astropart. Phys.* **11** (2010) 012.
- [72] V. K. Oikonomou, *Gen. Relativ. Gravit.* **47** (2015) 126.
- [73] K. Bamba, J. de Haro, and S. D. Odintsov, *J. Cosmol. Astropart. Phys.* **02** (2013) 008.
- [74] J. Amorós, J. de Haro, and S. D. Odintsov, *Phys. Rev. D* **87**, 104037 (2013).
- [75] S. Nojiri, S. D. Odintsov, and V. K. Oikonomou, *Phys. Lett. B* **775**, 44 (2017).
- [76] S. Nojiri, S. D. Odintsov, and V. K. Oikonomou, *Phys. Rep.* **692**, 1 (2017).
- [77] S. Nojiri and S. D. Odintsov, *Phys. Rep.* **505**, 59 (2011).
- [78] J. c. Hwang and H. Noh, *Phys. Rev. D* **71**, 063536 (2005).
- [79] H. Noh and J. c. Hwang, *Phys. Lett. B* **515**, 231 (2001).
- [80] J. c. Hwang and H. Noh, *Phys. Rev. D* **66**, 084009 (2002).
- [81] A. Ijjas, *J. Cosmol. Astropart. Phys.* **02** (2018) 007.
- [82] J. Quintin, Z. Sherkatghanad, Y. F. Cai, and R. H. Brandenberger, *Phys. Rev. D* **92**, 063532 (2015).
- [83] L. Battarra, M. Koehn, J. L. Lehnert, and B. A. Ovrut, *J. Cosmol. Astropart. Phys.* **07** (2014) 007.
- [84] O. E. Núñez, J. Socorro, and R. Hernández-Jiménez (Planck Collaboration), *Astrophys. Space Sci.* **364**, 69 (2019).
- [85] Y. B. Li, J. Quintin, D. G. Wang, and Y. F. Cai, *J. Cosmol. Astropart. Phys.* **03** (2017) 031.
- [86] S. Akama, S. Hirano, and T. Kobayashi, arXiv:1908.10663.
- [87] V. A. Belinskii, I. M. Khalatnikov, and E. M. Lifshitz, *Adv. Phys.* **19**, 525 (1970).
- [88] A. M. Levy, *Phys. Rev. D* **95**, 023522 (2017).
- [89] J. K. Erickson, D. H. Wesley, P. J. Steinhardt, and N. Turok, *Phys. Rev. D* **69**, 063514 (2004).
- [90] D. Garfinkle, W. C. Lim, F. Pretorius, and P. J. Steinhardt, *Phys. Rev. D* **78**, 083537 (2008).